HHS Public Access

Author manuscript

Neuropsychologia. Author manuscript; available in PMC 2018 January 27.

Published in final edited form as:

Neuropsychologia. 2017 January 27; 95: 156–172. doi:10.1016/j.neuropsychologia.2016.11.019.

An fMRI investigation of the relationship between future imagination and cognitive flexibility

R.P. Roberts[1], **K. Wiebels**[1], **R.L. Sumner**[1], **V. van Mulukom**[1,2], **C.L. Grady**[3], **D.L. Schacter**[4], and **D.R. Addis**[1,5]

[1]School of Psychology and Centre for Brain Research, The University of Auckland, Auckland, New Zealand [2]Centre for Research in Psychology, Behaviour and Achievement, Coventry University, Coventry, UK [3]Rotman Research Institute at Baycrest Hospital and Departments of Psychiatry and Psychology, University of Toronto, Toronto, Canada [4]Department of Psychology and Center for Brain Science, Harvard University, Cambridge, MA, USA [5]Brain Research New Zealand

Abstract

While future imagination is largely considered to be a cognitive process grounded in default mode network activity, studies have shown that future imagination recruits regions in both default mode and frontoparietal control networks. In addition, it has recently been shown that the ability to imagine the future is associated with cognitive flexibility, and that tasks requiring cognitive flexibility result in increased coupling of the default mode network with frontoparietal control and salience networks. In the current study, we investigated the neural correlates underlying the association between cognitive flexibility and future imagination in two ways. First, we experimentally varied the degree of cognitive flexibility required during future imagination by manipulating the disparateness of episodic details contributing to imagined events. To this end, participants generated episodic details (persons, locations, objects) within three social spheres; during fMRI scanning they were presented with sets of three episodic details all taken from the same social sphere (*Congruent* condition) or different social spheres (*Incongruent* condition) and required to imagine a future event involving the three details. We predicted that, relative to the *Congruent* condition, future simulation in the *Incongruent* condition would be associated with increased activity in regions of the default mode, frontoparietal and salience networks. Second, we hypothesized that individual differences in cognitive flexibility, as measured by performance on the Alternate Uses Task, would correspond to individual differences in the brain regions recruited during future imagination. A task partial least squares (PLS) analysis showed that the *Incongruent* condition resulted in an increase in activity in regions in salience networks (e.g. the insula) but, contrary to our prediction, reduced activity in many regions of the default mode network (including the hippocampus). A subsequent functional connectivity (within-subject seed PLS) analysis showed that the insula exhibited increased coupling with default mode regions during the *Incongruent* condition. Finally, a behavioral PLS analysis showed that individual differences in cognitive flexibility were associated with differences in activity in a number of regions from

Corresponding author: Reece Roberts, School of Psychology, The University of Auckland Private Bag 92019, Auckland 1142, New Zealand, r.roberts@auckland.ac.nz.

frontoparietal, salience and default-mode networks during both future imagination conditions, further highlighting that the cognitive flexibility underlying future imagination is grounded in the complex interaction of regions in these networks.

Keywords

autobiographical memory; cognitive flexibility; default mode network; divergent thinking; episodic simulation; frontoparietal control network; future thinking; salience network

1. Introduction

Much recent research has focused on the notion that the brain is a fundamentally prospective organ (Schacter, Addis, & Buckner, 2007), using information gleaned from the present environment and past memories to generate predictions about the future. Indeed, much of our time is consumed by various types of future-oriented thoughts that range in their depth and flexibility (Szpunar, Spreng, & Schacter, 2014). Like many species, humans can enlist inflexible reproductions of memorized or instinctual behaviors in a future-directed fashion (Suddendorf & Corballis, 2007). Humans, however, can also construct mental simulations of novel future events in sufficient detail to support effective planning (Buckner & Carroll, 2007; Gilbert & Wilson, 2007; Schacter, 2012; Schacter et al., 2012; Schacter & Addis, 2007). In fact, it is likely that the ability to simulate experiences beyond the immediate present environment underlies the human capacity to respond flexibly to unexpected changes in the environment (Buckner & Carroll, 2007; Suddendorf & Corballis, 2007).

The constructive nature of the episodic memory system (Bartlett, 1932; Schacter, Norman, & Koutstaal, 1998) makes it well-suited to support the construction of novel simulations. According to the constructive episodic simulation hypothesis (Schacter & Addis, 2007), the storage of episodic memories as a pattern of features distributed across the cortex (Damasio, 1989; Schacter et al., 1998; Squire, 1992) facilitates the extraction of episodic details—such as familiar people, places and objects—as content for simulations. Support for the idea that *access* to episodic memory is required for simulation comes from neuroimaging studies reporting that both memory and simulation engage a core network of regions overlapping substantially with the default mode network (DMN; Benoit & Schacter, 2015; Schacter et al., 2012; Schacter, Addis, & Buckner, 2007) as well as patient studies documenting corresponding deficits in episodic memory and simulation (Addis, Sacchetti, Ally, Budson, & Schacter, 2009; Addis, Wong, & Schacter, 2008; Andelman, Hoofien, Goldberg, Aizenstein, & Neufeld, 2010; Hassabis, Kumaran, Vann, & Maguire, 2007; Klein, Loftus, & Kihlstrom, 2002; Kwan, Carson, Addis, & Rosenbaum, 2010; but see also Squire et al., 2010). In addition to episodic memory, semantic memory also plays a critical role in future simulation, providing a scaffold for event representations (Irish & Piguet, 2013). Indeed, without access to semantic memory, future simulation is impaired (Duval et al., 2012; Irish, Addis, Hodges, & Piguet, 2012; Viard et al., 2014), and interestingly the network associated with semantic memory overlaps considerably with the DMN (Binder & Desai, 2011; Binder, Desai, Graves, & Conant, 2009; Burianova, McIntosh, & Grady, 2010) further suggesting a critical interplay between these systems during simulation.

According to the constructive episodic simulation hypothesis, extracted episodic details must also be *recombined* into a coherent event simulation. This recombinatory ability is thought to be central to *flexibly* imagining the future – to construct as well as disassemble and rework the components of scenarios to create different outcomes to enhance future behavior (Addis, Pan, Musicaro, & Schacter, 2016; Schacter & Addis, 2007). Despite this theoretical importance, little is known about the recombination process, including its neural correlates. Much of the existing evidence rests on neuroimaging reports of increased activity during the simulation of future events relative to remembering past events (e.g., Addis, Cheng, Roberts, & Schacter, 2010; Addis, Wong, & Schacter, 2007; Benoit & Schacter, 2015). Increased activity for future imagination relative to remembering the past has been interpreted as reflecting the recombination of episodic details into a coherent scenario because, by definition, the details comprising a novel event are less congruent than the details previously bound into a past event, and thus should impose higher demands on recombinatory processes. Regions across the DMN have been reported as exhibiting such effects, including frontopolar/dorsomedial and dorsolateral prefrontal cortex, lateral temporal and parietal cortex, precuneus, posterior cingulate, and hippocampus (Abraham, Schubotz, & von Cramon, 2008; Addis et al., 2010, 2007; Addis, Pan, Vu, Laiser, & Schacter, 2009; Gilmore, Nelson, & McDermott, 2016; Szpunar, Watson, & McDermott, 2007; Viard et al., 2011; for a meta-analysis, see Benoit & Schacter, 2015)

The hippocampus has been a focus in the study of recombination during simulation – perhaps unsurprising given the established role of this structure in relational processing, including the binding together of disparate elements during working memory as well as episodic encoding and retrieval (Axmacher et al., 2010; Eichenbaum, 2001; Hannula & Ranganath, 2008; Hannula, Tranel, & Cohen, 2006; Staresina & Davachi, 2009). Indeed, the simulations generated by hippocampal amnesics are not only sparse in episodic detail but also less coherent than those of healthy controls (Hassabis et al., 2007). Hippocampal amnesics are diminished in their ability to imagine future events that draw heavily on semantic information (e.g. the presidential election in 2032), suggesting the hippocampus may also play a role in the binding together of semantic details to produce complex semantic representations (Race, Keane, & Verfaellie, 2013). Moreover, simulation-related hippocampal activity is greatest when constructing future events for the first time (Gaesser, Spreng, McLelland, Addis, & Schacter, 2013; van Mulukom, Schacter, Corballis, & Addis, 2013), particularly when these events are specific in nature (Addis et al., 2010) and comprise greater amounts of detail (Addis & Schacter, 2008; Madore, Szpunar, Addis, & Schacter, 2016). These construction effects are evident even when controlling other possible determinants of hippocampal activity such as event novelty (Gaesser et al., 2013) and encoding (Martin, Schacter, Corballis, & Addis, 2011; for additional discussion see Schacter, Addis, & Szpunar, in press). Interestingly, Weiler, Suchan, & Daum (2010) found that simulating less probable events (that likely involve more incongruent combinations of details) engages the hippocampus more than commonplace, high probability events, although the disparateness of details was not directly measured.

This evidence, however, is limited in that these studies provide only *indirect* support of the recombination process; as yet, the effects of explicitly modulating recombinatory demands on simulation-related brain activity have not been investigated directly. Moreover, the focus

on the hippocampus has been at the expense of characterizing recombination effects in other DMN regions. Thus, the current study is the first to experimentally manipulate the disparateness of details comprising future simulations, thereby directly testing this hypothesized function of the hippocampus and exploring the effects on extra-hippocampal regions during future simulation.

In addition to recombinatory processes, we propose that successfully organizing disparate elements into a coherent scenario places demands on other domain-general processes supported by networks outside of the DMN. One such process is spontaneous cognitive flexibility (Eslinger & Grattan, 1993) which refers specifically to the ability to spontaneously generate a diversity of ideas (in contrast to reactive cognitive flexibility – the ability to shift mental set in response to changing environmental demands). Spontaneous cognitive flexibility (referred to hereafter as cognitive flexibility) involves the ability to "break conventional or obvious patterns of thinking" (Dietrich, 2004, p.1014) in the service of generating novel ideas, and as such can be indexed by divergent thinking[1] measures (Eslinger & Grattan, 1993; Tomer, Fisher, Giladi, & Aharon-Peretz, 2002), such as the flexibility measure of the Alternate Uses Task (AUT; Guilford, 1967). Indeed, this domain-general ability supports many forms of creative processing, including music, poetry and, relevant here, imagination (Beaty, Benedek, Silvia, & Schacter, 2016). Consistent with the notion that cognitive flexibility is important for recombining disparate details during simulation, Addis, Pan, Musicaro, & Schacter (2016) found that the amount of episodic detail comprising future simulations was positively associated with divergent thinking as measured by the AUT.

It is important to note that although divergent thinking has been linked with the DMN, in particular the temporal pole and hippocampus (e.g. Benedek, Jauk, Fink, et al., 2014; Ellamil, Dobson, Beeman, & Christoff, 2012; Takeuchi et al., 2011) this activity reflects the associative component of the task and is distinct from the executive component of the task – namely, cognitive flexibility – that is grounded in frontoparietal control network (FPCN) activity, especially lateral frontopolar cortex, including the rostrolateral prefrontal cortex (Benedek, Jauk, Sommer, Arendasy, & Neubauer, 2014; Gilhooly, Fioratou, Anthony, & Wynn, 2007; Niendam et al., 2012). Indeed, FPCN is particularly active during tasks that require cognitive flexibility and consistent with its domain-general role, the FPCN influences the activation of *other* task-specific networks (Cole et al., 2013). For instance, Beaty, Benedek, Kaufman, and Silvia (2015) found that FPCN regions (e.g., rostrolateral and dorsolateral prefrontal cortex) were functionally coupled with DMN regions during a divergent thinking task; moreover, the insula (part of the salience network, SN) was also coupled with the DMN in the early stages of the task, likely supporting the switching between large-scale networks (Menon & Uddin, 2010). In addition, the same study showed that more cognitively flexible individuals (i.e. those with the most creative responses in the AUT) exhibited increased coherence between FPCN and DMN regions. Additionally, it has been shown that during flexible future planning, the FPCN couples with DMN regions (Spreng, Stevens, Chamberlain, Gilmore, & Schacter, 2010), supporting the top-down

[1]While divergent thinking is often defined as synonymous with "creativity", in of itself, it is just one component of the creative thinking faculty, along with convergent thinking, working memory, sustained attention, etc. (Dietrich, 2004).

evaluation and modification of self-generated ideas to meet task-specific goals (Beaty et al., 2016).

Interestingly, in a recent meta-analysis of activation during future simulation, Benoit & Schacter (2015) report five clusters falling within the boundaries of the FCPN that exhibit greater activity when imagining the future relative to remembering the past. Thus, while it is clear that the FPCN is often recruited during future simulation, whether this is related to the degree of cognitive flexibility required by the simulation task remains unknown. We explored this question in two ways. First, our manipulation of detail disparateness should affect not only the demands placed on recombinatory process but also on cognitive flexibility. Specifically, recombining *incongruent* details in a meaningful way requires more cognitive flexibility than integrating *congruent* details, and thus under those task demands we expect to see not only activation the DMN, but also the FPCN (and the SN, supporting switching between these networks), as well as increased functional connectivity between these networks. Second, we investigated whether individual differences in cognitive flexibility (as indexed by divergent thinking) are related to brain activity while individuals are imagining the future.

To this end, we used a recently-developed version of the experimental recombination paradigm in which the disparateness of memory details to be incorporated into each imagined scenario was directly manipulated (van Mulukom, Schacter, Corballis, & Addis, 2016). Specifically, prior to scanning, participants generated lists of people, places and objects associated with distinct social spheres in their own lives (e.g., work, home, sports team). The key premise underlying this manipulation is that details from the same sphere (e.g., Brother, Nanna's House, Dad's car) are more congruent and more easily recombined into a scenario than are details from different spheres (e.g., Mum, Prof. Tulving's office, soccer ball). Participants' ratings on this task confirm that the social sphere manipulation affects the disparateness of details: within-sphere (congruent) details are rated as more likely to co-occur in everyday life than across-sphere (incongruent) details. Thus, unlike previous versions of the recombination paradigm where random sets of episodic details are presented during scanning (Addis, Pan, et al., 2009; Martin et al., 2011), in the current study participants were presented with *congruent* and *incongruent* sets of episodic details to incorporate into their future simulations; by experimentally manipulating the disparateness of the details to be included in an imagined scenario, we modulated the degree to which recombinatory and cognitive flexibility processes were required during future simulation. We also collected data on dimensions that potentially affect the intensity of simulation-related brain activity (i.e., encoding, detail, plausibility, novelty, difficulty) to enable us to isolate activation related to integration of disparate details.

We predicted that constructing future simulations from disparate details (*Incongruent* condition) would be associated with (1) increased activation of the DMN, including the hippocampus, reflecting increased recombinatory demands; (2) increased recruitment of the FPCN and SN, reflecting the executive functions underlying domain-general cognitive flexibility and (3) increased functional connectivity between SN, FPCN and DMN regions. Moreover, we investigated whether individual differences in cognitive flexibility (as indexed by the flexibility measure of the AUT) were related to activity in regions of both the DMN

and FPCN while individuals are imagining the future. We predicted that such brain-behavior relationships would be stronger in the *Incongruent* condition, as this condition should draw more heavily on associative processing (subserved by DMN regions) and executive function (FPCN regions) than the *Congruent* condition, and previous work has shown cognitive flexibility to be related to both associative and executive processing (Beaty, Silvia, Nusbaum, Jauk, & Benedek, 2014).

2. Methods

2.1 Participants

Twenty-five healthy young adults with no history of neurological or psychiatric conditions participated in this study, providing informed written consent in a manner approved by the University of Auckland Human Ethics Committee. All participants were fluent in English and right-handed (as determined using the Edinburgh Handedness Inventory; Oldfield, 1971). Data from two participants were excluded because they were unable to complete the fMRI scan, and one due to task non-compliance during the post-scan interview. Thus, data from 22 individuals (7 males; M_{age}=21.2, SD_{age}=3.74) were included in the analyses.

2.2 Tasks

2.2.1 Alternate Uses Task (AUT)—Divergent thinking was measured using the AUT (Guilford, 1967). On each of six trials, participants were required to generate as many alternate uses as possible for the given object (brick, button, automobile tyre, key, pencil, and paperclip). Each trial was three minutes in duration; at the two minute mark, participants were alerted that they had one minute remaining. Participant responses were recorded, transcribed and scored for flexibility—the number of distinct categories their responses for an item could be grouped into—by two independent coders. For example, on the trial *paperclip*, the responses ‘to make a bracelet’, ‘to make a ring’, and ‘to make earrings’ would all be grouped together in one category, and the response ‘to use as mini rodent ice skates’ in another, resulting in a flexibility score of 2. For each participant, the total flexibility score summed across the six trials was used for analysis. Two independent raters scored all responses; a two-way mixed model confirmed a high degree of inter-rater reliability (standardized Cronbach’s alpha = .97).

2.2.2 Future Simulation fMRI Task—During a pre-scan session, participants were asked to identify three distinct social spheres (e.g. university, work, family etc.) For each sphere, they provided a list of 40 persons, locations and objects encountered within the last 5 years. No detail could be duplicated across spheres, and any person that the participant indicated could be placed into more than one sphere was removed. Each detail was then rated for familiarity (0=only encountered once; 3=as familiar as a parent or spouse) and frequency of encounter (0=encountered annually; 1=monthly; 2=weekly, 3=daily). The person, location and object details were then used to create 45 person/place/object detail sets for each of two conditions: (1) *Congruent*, where the 3 details comprising a detail set were from the same sphere; and (2) *Incongruent*, where each detail comprising a detail set came from a different sphere. Mean familiarity and frequency of encounter ratings of details comprising congruent

and incongruent sets were matched across the two conditions (familiarity: $t_{21} = .27$, $p = .793$; frequency of encounter; $t_{21} = .54$, $p = .598$).

For each future simulation trial during scanning, participants were presented with a detail set on the screen (i.e., three words that corresponded to a person, location and object) from the *Congruent* or *Incongruent* condition (10 *s*); the order in which the person, place and object details were presented was counterbalanced across trials. Participants were instructed to imagine, from a field perspective (i.e., "through their own eyes"), a specific future event that could occur within the next 5 years that incorporated the three details. Once they had an event in mind, participants made a button press and then elaborated the event for the remainder of the trial. Each trial was followed by a rating scale (4 *s*) for the amount of detail comprising the simulation (0 = little or no detail, 3 = vivid detail).

Immediately following the scan, participants completed a post-scan session in two parts. First, to measure degree of encoding of simulations generated during scanning, participants completed a cued-recall test for detail sets shown in the future task (Martin et al., 2011); for each set, two details were presented and they had to recall the third missing detail. The test was self-paced and the type of detail to be recalled (person, location, object) was counterbalanced across trials. Second, participants were presented with each complete detail set and asked to briefly describe the future event they had generated during the scanner. This description was used to confirm that the event was future-oriented, self-relevant (i.e., they imagined themselves in the event) and specific in time and place; any trials for which this was not the case were dropped from further analyses. Participants provided an estimated date for each future event (in years). They also rated the plausibility of the event (0 = very implausible; 3 = very plausible), its novelty assessed by rating the similarity of the event to previously experienced or imagined events (0 = not at all similar; 3 = very similar) and how difficult it was to construct the simulation (0 = not at all difficult; 3 = very difficult). To confirm our manipulation of detail disparateness, participants rated each detail set for how likely the three details would be to co-occur in everyday life (0 = not at all likely; 3 = very likely).

2.2.3 Control fMRI Task—The scanning session also included 45 trials of a sentence construction control task that involved retrieval of semantic information and visual imagery (Addis, Pan, et al., 2009). A list of 27 highly familiar (M = 5.48, SD = 1.01), imageable (M = 6.44, SD = 0.27) and concrete (M = 6.94, SD = 0.06) nouns was compiled from the Clark and Paivio (2004) extended norms. For each trial, three nouns were randomly selected from this list and presented (10 *s*). Participants made a size judgement by generating a sentence in the form of '*X is bigger than Y, which is bigger than Z*' (e.g. 'car is bigger than bag, which is bigger than phone'). Once constructed, they made a button press and focused on the semantic definition of each noun for the remaining time. Participants then rated the difficulty they had constructing the sentence (0 = very easy, 3 = very difficult; 4 *s*).

2.3 Scanning Session

Participants completed 7 practice trials (4 simulation trials and 3 control trials) outside of the scanner; participants were ask to describe the simulations they generated on these trials to

confirm they understood the task instructions (i.e., that they were imagining future scenarios that involved themselves and doing so from a field perspective).

Participants completed five runs of functional scanning, each 482 *s* in duration. Each run comprised 18 future simulation trials (half *Congruent* and half *Incongruent*) and 9 control trials. Null trials (fixation cross) comprised 22% (104 *s*) of each run. The randomized order of all trials, and the jittered duration of null trials, was determined using Optseq 2.0 (Dale, 1999).

2.3.1 MRI Acquisition Parameters—MRI data were acquired on a 3T Siemens MAGNETOM Skyra scanner. Anatomical scans were acquired using a magnetization prepared rapidly acquired gradient echo (MP-RAGE) sequence. Whole-brain functional scans were acquired using a T2*-weighted echo planar imaging (EPI) sequence (TR = 3000 ms, TE = 27 ms, FOV = 225 mm, flip angle = 90°) with 59 coronal-oblique slices (3.5 mm) acquired in an interleaved fashion at an angle perpendicular to the long axis of the hippocampus. Field maps were acquired using Siemens standard double-echo field map sequence (TR = 577ms; TE = 4.92 and 7.38ms). Task stimuli (black text on white background) were projected onto a mirror incorporated into the 20-channel head coil. E-Prime software (Psychology Software Tools, Inc., Pittsburgh, P.A.) was used for timed presentation of stimuli and collection of participants responses made via a 4-button MR-compatible response box.

2.4 Procedure

Participants completed three sessions, spaced approximately one week apart. During Session 1, participants provided person, location and object details for the future simulation tasks. During Session 2, participants completed the AUT. During Session 3, participants completed the scanning session and post-scan interview.

2.5 Data Analysis

2.5.1 Trial Selection—Any trials on which no response was recorded or response times were less than 500ms were excluded from further analysis. In addition, any future trials for which no specific event could be described during the post-scan interview were excluded.

2.5.2. Behavioral Analyses—Paired *t*-tests and analyses of variance (ANOVA) were used as appropriate to assess effects of condition on behavioral measures. For ANOVAs, if the assumption of sphericity was violated ($\varepsilon < .90$), a correction factor to account for the inflation in Type I error rate was applied to the degrees of freedom of the F-distribution (Geisser & Greenhouse, 1958). Pearson correlations were performed between AUT flexibility scores and *Incongruent-Congruent* difference scores for the following behavioral measures: construction response time, subsequent memory (proportion correct), and subjective ratings (difficulty, plausibility, detail and novelty). We used difference scores due to the subjective nature of the ratings; if different participants use the rating scales differently, it could obscure any relationships between the AUT flexibility scores and the behavioral ratings, rendering the results difficult to interpret. However, any given participant is unlikely to use the rating scale differently for the *Congruent* and *Incongruent* conditions,

rendering difference scores as most appropriate for this analysis. We predicted that highly flexible individuals will show less of a *Congruent-Incongruent* difference in subjective ratings conditions (i.e., a negative relationship between behavioral difference scores and flexibility scores). For example, relative to someone low in cognitive flexibility, a highly flexible individual is predicted to experience a smaller shift in difficulty (or any of the dimensions) between the *Congruent* and *Incongruent* conditions.

2.5.3 Preprocessing—The first four images from each run were discarded to allow the longitudinal magnetization to reach equilibrium. Functional images were preprocessed using SPM8 (Wellcome Trust Centre for Neuroimaging, London, UK). Preprocessing included slice-time correction, correction for motion and distortion (using SPM8's Realign and Unwarp routine together with the Field Map toolbox (Hutton et al., 2002), co-registration with the anatomical scan, spatial normalization using parameters derived during segmentation to the Montreal Neurological Institute (MNI) template (resampled at 2×2×2 mm voxels) and spatial smoothing (8mm full-width half maximum Gaussian kernel).

2.5.4 Spatiotemporal Partial Least Squares (ST-PLS)—Event-related functional data were analyzed using a ST-PLS approach, a multivariate approach used extensively in studies on autobiographical memory and future simulation (e.g. Addis, McIntosh, Moscovitch, Crawley, & McAndrews, 2004; Addis, Roberts, & Schacter, 2011; Addis, Pan, et al., 2009; Burianova & Grady, 2007; Burianova et al., 2010; Martin et al., 2011; Spreng & Grady, 2010). Partial least squares (PLS) offers more power than univariate approaches; unlike univariate approaches where a separate statistical analysis is computed at every voxel, PLS is a multivariate technique and so all voxels are included one analysis. Therefore, a correction for multiple comparisons is not required. It also makes no assumptions about the shape and time course of the hemodynamic response function (HRF).

2.5.4.1 Task PLS Analyses: Data were analyzed using non-rotated task ST-PLS analyses over a temporal window of 5 TRs (15 *s*). A data matrix comprising blood-oxygenation level dependent (BOLD) signal from all participants and all voxels (within a custom-made gray matter mask derived by segmenting an MNI brain and binarizing the resulting gray matter image) for specified conditions at each TR in this temporal window was constructed; for each trial, BOLD signal data from TRs in the temporal window were normalized relative to the signal at the onset of the trial. The data matrix was cross-correlated with the design matrix (comprising vectors specifying *a priori* contrasts of conditions). The resultant cross-product matrix underwent singular value decomposition, producing latent variables comprised of: (i) a singular value indicating the amount of covariance for which the LV accounts; (ii) a linear contrast across conditions that codes for the effect depicted by voxels; and (iii) a singular image of voxel weights ("saliences") that indicates the voxels exhibiting the greatest covariance with the linear contrast during each TR. The weighted value of a salience can be either positive or negative, depending on its relation to the specified contrast of conditions. Brain scores (a weighted average of all voxel saliences associated with a condition) were also derived for each participant in each condition, specifying how strongly the spatiotemporal brain pattern for a given LV is expressed by that participant.

The overall statistical significance of each LV was determined using permutation testing (1000 permutations). For each permutation, all participants' data were reassigned to conditions, the ST-PLS was re-run and a new singular value obtained. Significance indicated the probability of the number of times the singular value from the permuted data exceeded the actual singular value (McIntosh, Bookstein, Haxby, & Grady, 1996); a threshold of $p < .05$ was used. Note that because PLS is a multivariate technique, all voxels are included in the same analysis and thus because only one analysis is computed, the need to correct for multiple comparisons is obviated[2].

Bootstrapping estimation of the standard error (SE) was used to determine the reliability of voxel saliences; participants were randomly resampled with replacement, the ST-PLS was re-run and the saliences computed. After this procedure was completed 1000 times, the SE of the saliences was computed. Voxels in which bootstrap ratios were greater than ±3.00 (roughly equivalent to $p < .001$) were considered to represent reliable voxels; only clusters of 10 or more voxels are presented for brevity. Confidence intervals for brain scores (which are based on saliences) were also calculated using this procedure. Examination of 95% confidence intervals around brain scores provides an indication of whether a condition reliably contributes to the spatiotemporal pattern associated with the contrast (as indicated by confidence intervals that do not include zero) and whether the conditions contributed differentially to the pattern (as indicated by non-overlapping confidence intervals).

As is common practice in studies using event-related PLS (e.g., Addis et al., 2004, 2011; Hirshhorn, Grady, Rosenbaum, Winocur, & Moscovitch, 2012), we report results from TRs in which the effects were maximal (i.e., the TRs at which the spatial pattern comprised the greatest number of voxels); focusing on maximal TRs has the benefit of brevity while still providing critical insights into the spatial patterns and temporal trajectories associated with the conditions. The MNI co-ordinates of the peak voxels within each cluster were localized using Harvard-Oxford Atlases (Desikan et al., 2006). In addition, each cluster was localized to functional networks by determining each cluster's degree of overlap with the seven network cortical parcellation of (Yeo et al., 2011; available from https://surfer.nmr.mgh.harvard.edu/fswiki/CorticalParcellation_Yeo2011), allowing us to determine which clusters belonged to the DMN, FPCN and SN. For illustrative purposes, singular images were overlaid on the MNI ICBM 152 nonlinear anatomical template image (Fonov et al., 2011) and percent signal change values from the peak voxels of clusters in the DMN, FPCN and SN were extracted and plotted for illustrative purposes.

Using the above-described ST-PLS procedure, we ran a series of analyses; for each, the relevant *a priori* contrast of conditions was specified. (1) The first analysis contrasted the two future conditions relative to the control task as a data quality check; as the results replicated previous findings (i.e., significant activation of the default mode network during future simulation), these result are not discussed any further. (2) The second analysis contrasted *Congruent* and *Incongruent* future events to test our main hypotheses. However, as the two conditions differed along a range of phenomenological dimensions (detail,

[2]In contrast to the multivariate approach where data from all voxels are included in the same analysis, the univariate approach requires multiple statistical analyses be computed (one at each voxel), thus requiring a correction for multiple comparisons.

plausibility, novelty, difficulty) and on levels of encoding (i.e., performance on the cued-recall test; see ***Section 3.1***), it could be the case that any activation differences between the *Congruent* and *Incongruent* conditions simply reflected differences in these behavioral dimensions rather than the experimental manipulation *per se*. To determine which clusters of activation were affected by these behavioral variables, we computed Analysis 2 five times, each time using functional data that had been residualized for the effect of one of these covariates (detail ratings, plausibility ratings, novelty ratings, difficulty ratings, encoding success - proportion correct) as described below (Section 2.5.4.2). Thus, we restricted our reporting of Analysis 2 to only those clusters that were evident in each of the five analyses using residualized data.

2.5.4.2 Residualization Procedure for Task PLS: Because the *Congruent* and *Incongruent* conditions differ on a number of behavioral dimensions that could influence relevant brain activity, we developed a residualization procedure for task PLS analyses to correct the BOLD data for these differences. Specifically, we removed variance that was shared by (i) *Congruent-Incongruent* differences in behavioral scores, AND (ii) *Congruent-Incongruent* differences in BOLD signal (Wiebels, Roberts, & Addis, 2016). We could have opted to run the residualization procedure separately for each condition, but controlling for behavior within each condition separately is confounded by between-subject variability associated with both behavioral responses and the BOLD signal. In the current study, a potential source of between-subject variability in the behavioral data is the use of subjective rating scales that can be interpreted differently by different participants. Importantly, however, any given participant is unlikely to use a rating scale differently across conditions. Likewise, some of the between-subject variance in the amplitude of the BOLD signal is likely to derive from sources that vary across participants but are unrelated to the experimental conditions (e.g., physiological factors; Dubois & Adolphs, 2016).

Thus, based on the logic of repeated-measures ANOVA (where between-subject variance is removed from the error term), we used *Congruent-Incongruent* difference scores so as not to confound our residualization with between-subject variability. We reasoned that if a *Congruent-Incongruent* activation difference is driven by a difference in behavior between the two conditions, there should be a linear across-subject relationship between these two sets of difference scores. For example, if the plausibility of simulated events is driving BOLD activity in a region, it should be the case that individuals with greater differences in plausibility ratings between the two conditions should also exhibit greater differences in BOLD activation between the conditions. Importantly, simply regressing out the effects of behavior for each condition separately does not necessarily remove the shared variance associated with a linear relationship between BOLD and behavior difference scores (see Supplementary Materials, Section S1, for a more detailed explanation of this point).

To regress out the behavioral differences from differences in fMRI data, difference scores were calculated for each TR at each voxel for each subject, creating vectors of difference scores (Eq. 1). Likewise, difference scores were calculated for the following behavioral scores: detail, plausibility, difficulty, novelty and encoding (Eq. 2).

$$\overrightarrow{\mathrm{BOLD}}_{\mathrm{Diff}}=\overrightarrow{\mathrm{BOLD}}_{\mathrm{Congruent}}-\overrightarrow{\mathrm{BOLD}}_{\mathrm{incongruent}} \quad \text{(Eq.1)}$$

$$\overrightarrow{\mathrm{Behav}}_{\mathrm{Diff}}=\overrightarrow{\mathrm{Behav}}_{\mathrm{Congruent}}-\overrightarrow{\mathrm{Behav}}_{\mathrm{incongruent}} \quad \text{(Eq.2)}$$

Separately, each behavioral difference score was regressed out of the BOLD differences, resulting in a difference between *Congruent* and *Incongruent* for each voxel at each TR that was independent of any differences in behavioral scores between the two conditions (Eq. 3).

$$\overrightarrow{\mathrm{BOLD}}_{\mathrm{Resid\ \ Diff}}=((I-\overrightarrow{\mathrm{Behav}}_{\mathrm{Diff}}*\overrightarrow{\mathrm{Behav}}_{\mathrm{Diff}}{}^{T}*\overrightarrow{\mathrm{Behav}}_{\mathrm{Diff}})^{-1}*\overrightarrow{\mathrm{Behav}}_{\mathrm{Diff}}{}^{T})*\overrightarrow{\mathrm{BOLD}}_{\mathrm{Diff}})+p$$
$$*I=\mathrm{identity\ \ matrix};p=\mathrm{intercept\ \ of\ \ regression\ \ line};T=\mathrm{transposed} \quad \text{(Eq. 3)}$$

Next, these residualized difference scores were projected back onto the original data matrix by subtracting them from the original percent signal change values in the *Congruent* condition (Eq. 4). This created a new set of percent signal change values for the *Incongruent* condition, by replacing the original difference between the two conditions with a difference that showed no relationship to the difference between the conditions on a given behavioral score. For a graphical description of this process, please see Supplementary Materials (Section S2).

$$\mathrm{BOLD}_{\mathrm{Resid\ \ incongruent}}=\mathrm{BOLD}_{\mathrm{Congruent}}-\mathrm{BOLD}_{\mathrm{Resid\ \ Diff}} \quad \text{(Eq.4)}$$

2.5.4.3 Seed PLS Analyses: To further explore the results of the *Incongruent-Congruent* Task PLS analysis, we assessed the functional connectivity of regions of interest within the FPCN and SN (i.e., FPCN: dorsolateral and rostrolateral prefrontal cortex; SN: insula, anterior cingulate cortex; Beaty et al., 2015) with the DMN, with the hypothesis that these regions reflecting domain-general cognitive flexibility will be more strongly coupled with the DMN during the Incongruent condition. Task-related functional connectivity was assessed for any regions of interest that were evident in the results of the Incongruent>Congruent task PLS analysis. To this end, we computed task-related functional connectivity using a novel version of seed PLS which we call within-subjects seed PLS (ws-seed PLS) that assesses temporal, within-subject correlations between a seed region and the rest of the brain (Roberts, Hach, Tippett, & Addis, 2016)[3]. Briefly, ws-seed PLS involves

[3]Standard seed PLS analyses involves taking voxels' mean percent signal change values and performing atemporal, across-subject correlations between the seed and the rest of the brain. As we have shown (Roberts, Hach, Tippett, … Addis, 2016), within- and across-subject correlations of BOLD data often produce different findings, meaning that standard seed PLS results are not necessarily informative of the temporal interaction between brain regions.

calculating the mean BOLD signal for each trial in each voxel, thereby creating a vector of BOLD signal values for each voxel in each condition. This is similar to the beta-series correlation approach (Rissman, Gazzaley, & D'Esposito, 2004), except that the "series" are BOLD percent signal change values and not beta values derived from the general linear model. For each future simulation condition, these vectors were then correlated with the vector of BOLD signal values from the seed region (a 6mm cube comprising 27 voxels centered on the peak voxel in the left insula, *xyz* −38 4 14), creating a within-subject correlation coefficient for each voxel of the brain specifying the strength and direction of the temporal correlation of each voxel with the seed region. These seed-brain correlation coefficients were then submitted to a singular value decomposition to produce latent variables specifying task-related differences and similarities in functional connectivity between the seed and the rest of the brain. Permutation testing and bootstrapping procedures were conducted as described above in ***Section 2.5.4.1***, and results were thresholded using a BSR of ±3.00 (roughly equivalent to $p < .001$) and a spatial extent threshold of 10 voxels.

2.5.4.4 Behavior PLS: To identify regions in which task-related activity correlated with divergent thinking, a behavior PLS analysis on BOLD data from the two future simulation tasks was conducted. Specifically, for each task, BOLD signal from every voxel was correlated with a vector containing AUT flexibility scores in an across-subject fashion. These brain-behavior correlation coefficients were then submitted to a singular value decomposition, producing latent variables specifying task-related differences and similarities in correlations between activity and AUT flexibility scores. Permutation testing and bootstrapping procedures were conducted as described above in ***Section 2.5.4.1***, and results were thresholded using a BSR of ±3.00 (roughly equivalent to $p < .001$) and a spatial extent threshold of 10 voxels.

3. Results

3.1 Behavioral Results

The number of trials and response time (RT) data for all conditions, and the phenomenological measures for the two future simulation conditions, are presented in Table 1. For all conditions, only trials on which a RT was recorded or with RTs greater than 500ms were analyzed. An average of 1.64 and 2.82 trials per participant were excluded for the *Congruent* and *Incongruent* conditions respectively on this basis. For simulation trials, analysis was further restricted to include only those trials for which a specific event was recounted during the post-scan interview. The resulting bin sizes differed by condition ($F_{1.29,27.14}$=29.35, p<.001, η^2 = .59): there were more trials in the control condition than the future conditions (p values < .001), and the *Congruent* condition had more trials than the *Incongruent* condition ($p < .001$).

An ANOVA on RT data resulted in a main effect of condition ($F_{1.14,23.99}$=32.39, p<.001, η^2 = .61). Pairwise comparisons indicated that average RTs were faster in the control relative to future conditions (p values < .001). Although RTs in the *Congruent* future condition were significantly faster than RTs in the *Incongruent* condition (t_{21}=−3.32, p = .003, r^2=.34), the size of this difference was small relative to the duration of the trial (5 *s*) and the TR (3 *s*).

Thus, it is unlikely that this RT difference affected any differences between the estimated HRFs of the two conditions.

Phenomenological data are also presented in Table 1. In line with our manipulation, the within-sphere details comprising *Congruent* detail sets were rated as significantly more likely to co-occur than the across-sphere details comprising the *Incongruent* detail sets (t_{21}=7.68, $p < .001$, r^2=.74). The estimated temporal distances of *Incongruent* future events were slightly further from the present than *Congruent* events although this difference was not significant (t_{21}=−1.81, $p < .085$, r^2=.13) and the averages for both conditions were well within the 5 year limit imposed on participants.

Future simulations constructed in the *Incongruent* condition were rated by participants as more difficult to construct (t_{21}=−5.43, $p < .001$, r^2=.58), less similar to previous events (t_{21}= −5.91, $p < .001$, r^2=.62), less plausible (t_{21}=8.49, $p < .001$, r^2=.77), and less detailed (t_{21}=3.51, $p = .002$, r^2=.37) than events in the *Congruent* condition. Moreover, the proportion of detail sets correctly remembered during the cued-recalled test was lower in the *Incongruent* condition (t_{21}=6.28, $p < .001$, r^2=.65).

Finally, we computed correlations between AUT flexibility scores and each of the difference scores between Congruent and Incongruent condition (i.e., for each behavioral measure). These analyses revealed significant negative correlations of flexibility scores with difficulty ($r = -.49$, $p = .02$) and plausibility ($r = -.53$, $p = .01$) difference scores. While the relationship between flexibility scores and detail difference scores was also negative, this effect was not significant ($r = -.31$, $p = .16$). Novelty and encoding difference scores were not correlated with flexibility scores (novelty r = 0.07, encoding r = 0.00; both p values > 0.70).

3.2 Task PLS Results

The non-rotated task PLS analysis examining *Incongruent* versus *Congruent* future simulations produced a significant latent variable ($p < .001$), showing distinct whole-brain patterns of activity associated with each future simulation condition across the temporal window (5 TRs). As shown in Figure 1, positive brain scores (weighted averages of activity across all voxels associated with each task) and positive saliences were associated with regions in which BOLD signal was greater in the *Congruent* condition, while negative brain scores and saliences were associated with regions in which BOLD signal was greater for the *Incongruent* condition. As shown in Figure 2, the number of voxels responding to *Congruent* and *Incongruent* conditions varied across the temporal window, with the greatest number of significant voxels (thresholded at a BSR of ±3) showing a *Congruent* > *Incongruent* effect at TR 4 (9–12 *s* into the trial). Inversely, the TR in which the greatest number of voxels showed an *Incongruent* > *Congruent* effect was earlier in the temporal window (TR 2, 3–6 *s* into the trial). The effects at these maximal TRs are described in more detail below. Importantly, only those regions that are evident following the residualization of BOLD data for differences in all five behavioral dimensions (**Section 2.5.4.2)** are reported below so as to restrict our description of results to those regions showing effects *independent* of differences in behavior (see **Section S3** for the results of the task PLS analysis computed on raw (i.e., unresidualized) BOLD data and clusters affected by each residualization procedure; see

Figure S7 for a graphical depiction of the effect of the residualization procedure on activation).

3.2.1 TR 2—During TR 2 (3–6 *s* into the trial), the *Incongruent* condition was associated with increased BOLD responses relative to the *Congruent* condition in a number of regions that were largely outside the core network/DMN network (see Table 2A). Specifically, a number of regions in the SN were responsive to the increased constructive demands of the *Incongruent* condition. To interrogate these effects more closely, percent signal change values were extracted from peak voxels of selected clusters and plotted.

The region in which the *Incongruent* > *Congruent* effect was the most robust was in the left anterior/mid insula (*xyz* −38 4 14). As shown in Figure 3A, the effect in this region was characterized by a relative reduction in deactivation for the *Incongruent* condition. That is, while both conditions resulted in a reduction in a BOLD signal in this region relative to the start of the trial, this deactivation was less marked for the *Incongruent* condition. Likewise, as shown in Figure 3B, the supramarginal gyrus showed a similar effect with the *Incongruent* condition exhibiting slight activation compared to the deactivation observed in the *Congruent* condition at this early point in the temporal window. Conversely, there were some clusters outside the SN (e.g. fusiform gyrus and subcallosal cortex, Figures 3C and D) that exhibited greater activations (i.e., positive percent signal change relative to the start of the trial) during the *Incongruent* relative to *Congruent* condition. Clusters in DMN regions (middle temporal gyrus, medial parietal and medial frontal cortices) showed increased activity in the *Congruent* condition at this time-point. In addition, a cluster in part of the SN, the right insula, showed reduced deactivation in the *Congruent* condition relative to the *Incongruent* condition.

3.2.2 (TR 4)—Contrary to our hypothesis, it was the *Congruent* condition that resulted in increased activation of the core network/DMN relative to the *Incongruent* condition (see Table 2D). A single, massive cluster of activation (> 10,000 voxels), with a peak voxel located in the left cerebellum, extended bilaterally into medial parietal (retrosplenial cortex, posterior cingulate and precuneus) and medial temporal cortices. In addition, bilateral lateral temporal cortices and the right angular gyrus also showed this *Congruent>Incongruent* effect. As shown in Figure 4, percent signal change extracted from peak voxels of clusters showed that while both conditions recruited the DMN, this effect was significantly more pronounced for the *Congruent* condition. It is important to note that while the responses to the *Congruent* condition were greater in magnitude, most of these key DMN regions (shown in Figure 4) also showed reliable responses to the *Incongruent* condition (i.e. one-sample *t*-tests confirmed percent signal change values at TR 4 to be significantly different from zero; all *p* values < .02). The exception to this finding was in the left hippocampus, in which the *Incongruent* condition elicited percent signal change values that were not reliably different from zero ($p > .09$). In addition to the DMN, the *Congruent* condition also produced increased activation in some regions in the FPCN (e.g. right middle frontal gyrus, superior parietal lobule) and SN (e.g. right insula, bilateral precentral gyrus). At this TR, a single cluster, located in the left insula showed a reliable Incongruent > Congruent effect; this

cluster was the same locus of activity as the left insula cluster showing the same effect at TR2.

3.3 Seed PLS – Left Insula

We were interested in examining the functional connectivity of regions of interest in the FPCN (dorsolateral and rostrolateral prefrontal cortex) and SN (insula, anterior cingulate cortex) associated with the *Incongruent* condition, in line with previous reports of these regions coupling with the DMN during tasks that require increased cognitive flexibility (Beaty et al., 2015). The only one of these regions to exhibit an *Incongruent* > *Congruent* effect was the insula. Specifically, during both TRs 2 and 4, the left mid-anterior insula (*xyz* −38 4 14) showed reduced deactivation during the *Incongruent* condition relative to the *Congruent* condition. A mean-centered ws-seed PLS analysis on the *Congruent* and *Incongruent* conditions produced a significant LV ($p < .005$) indicating reliable whole-brain differences between the two conditions in functional connectivity with a $6mm^3$ ROI centered on the left mid-anterior insula (*xyz* −38 4 14). As shown in Figure 5, during the *Incongruent* condition the insula seed showed differential functional connectivity with two DMN regions: the left temporal pole (*xyz* −56 8 −30) and the right angular gyrus (*xyz* 50 −62 28) (see Table 3). In addition, a cluster in the left parahippocampal gyrus (*xyz* −22 −26 −24) also showed the same effect, but failed to meet the chosen cluster size threshold of 10 voxels. The seed region did not show preferential functional connectivity to any regions in either the SN or the FPCN. During the *Congruent* condition, increased functional connectivity with the left insula seed was most prominent in a large bilateral prefrontal cluster (maximal in left dorsolateral prefrontal cortex) that extended into the anterior cingulate cortex.

3.4 Behavior PLS – Cognitive Flexibility

A behavior PLS analysis using AUT flexibility scores was computed to identify regions in which activity during future simulation correlated with divergent thinking abilities – an index of cognitive flexibility. This analysis yielded a significant LV ($p < .05$) explaining 70.46% of the crossblock covariance, revealing a set of brain regions linearly associated with AUT flexibility scores similarly for *both* future simulation tasks (see Figure 6). As for the task PLS analyses, we again restricted our description of results to the TR in which the greatest number of significant voxels was apparent: TR 3 in this case. During this time-window, AUT flexibility scores showed reliable correlations—both positive and negative—with BOLD signal in regions from various functional networks. As shown in Figure 7 and Table 4, AUT flexibility scores were positively associated with bilateral rostrolateral prefrontal cortices (*xyz* −20 62 10; 24 60 16), with these clusters extending into both the DMN and FPCN. Likewise, signal in the right temporal pole (DMN: *xyz* 52 4 −18) during the future simulation tasks showed a positive association with AUT flexibility scores. Inversely, a cluster in the left hippocampus (DMN: *xyz* −30 −28 −16) was negatively associated with AUT flexibility scores. Lateral prefrontal cortices (FPCN: *xyz* −46 38 8; 46 44 12) as well as bilateral amygdalae (*xyz* −32 −4 −24; 30 0 −26) also showed a negative association with cognitive flexibility.

4. Discussion

The current study investigated the neural correlates of recombinatory demands during the flexible simulation of future events using two approaches. First, we experimentally increased recombinatory demands during the simulation process by manipulating the disparateness of episodic memory details comprising an imagined future scenario, and assessed changes in both mean BOLD signal (Task PLS) and functional connectivity (ws-seed PLS) induced by this manipulation. Second, to determine if and how individual differences in cognitive flexibility relate to brain activity while imagining future scenarios, we performed brain-behavior correlations (Behavioral PLS) between flexibility scores from a divergent thinking task (AUT) and brain activity during future simulation.

Given that the hippocampus has previously been characterized as a key structure involved in the recombination of memory details during episodic future simulation (Addis & Schacter 2012; Benoit & Schacter, 2015), we predicted that increasing the disparateness of memory details (and hence increasing the demand placed on recombinatory processes) during the *Incongruent* condition should be associated with increased hippocampal activity as compared with the *Congruent* condition. Instead, our results showed that the *Congruent* condition resulted in stronger activation in a number of key DMN regions, including the hippocampus. This is particularly surprising, as Weiler et al. (2010) reported that right anterior hippocampal activity increased linearly as the plausibility of events decreased. There are, however, important differences between the two studies. In our study, participants were presented with three details that were to be integrated into imagined events, while Weiler et al. (2010) presented generic event cues (e.g. “Christmas dinner”). A consequence of this difference in experimental paradigm is that the episodic details retrieved and then recombined in the Weiler et al. study were internally generated, while our paradigm imposed additional constraints on the content of imagined scenarios. An effect of this manipulation was that the events in our study—even those in the *Congruent* condition—were rated as considerably less plausible than the events generated in the Weiler et al. study. This suggests that the linear relationship between plausibility and hippocampal activity observed in the Weiler et al. study may not hold for the entire spectrum of plausibility. Instead, extremely implausible events may be associated with decreased hippocampal activity (relative to less implausible events), as observed in the current study where hippocampal activity was reduced in the *Incongruent* condition.

As the epoch in which the *Congruent* > *Incongruent* effect was greatest (9–12 *s* into the trial) corresponded to the elaboration phase of the imagined scenario (Addis et al., 2007), a plausible interpretation of the increased hippocampal activity during the *Congruent* condition is that it reflects increased episodic memory retrieval, rather than recombination demands: perhaps due to the strong episodic associations between the congruent details comprising these events, more episodic information was retrieved, contributing to the generation of more elaborate imagined scenarios (as confirmed by higher detail ratings for *Congruent* simulations). By this account, the related details act as strong cues for the hippocampus to retrieve additional memory details associated with the three presented details (i.e. pattern completion; McClelland, McNaughton, & O’Reilly, 1995; Norman & O’Reilly, 2003). This proposal also bears resemblance to the notions of spreading activation

(Conway and Pleydell-Pearce, 2001) and autobiographical memory chaining (Mace, 2014), whereby retrieval of autobiographical memories triggers the automatic activation or retrieval of related memories. In addition, any increase in the number of memory details retrieved during the *Congruent* condition would also, necessarily, result in an increase in the recombinatory load associated with that condition, resulting in greater hippocampal activity. By this account, the recombinatory processes carried out by the hippocampus are determined not only by the novelty or disparateness of the memory details comprising an event (greater in the *Incongruent* condition), but also the number of details contributing the event (greater in the *Congruent* condition). Note also that this view is consistent with and indeed emerges from the multi-component model of hippocampal contributions to episodic future simulation put forth by Addis and Schacter (2012), which links the hippocampus with distinct components of future simulations, including both retrieval of episodic details and recombining those details.

Although the *Incongruent* condition was associated with less activation of the hippocampus and other DMN regions relative to the *Congruent* condition, we did find that the *Incongruent* condition was accompanied by recruitment of SN regions earlier in the trial (TR 2), which was in line with our hypothesis. This effect of reduced deactivation was most prominent in the left mid-anterior insula, a region previously shown to be strongly associated with task difficulty and error-monitoring (Bastin et al., 2016; Eckert et al., 2009; Kosillo & Smith, 2010; Taylor, Stern, & Gehring, 2007; Tregellas, Davalos, & Rojas, 2006). That the effect in the left insula survives residualization for behavioral and phenomenological differences suggests, however, that this region plays an active role in the recombination of disparate autobiographical details as opposed to merely signaling shifts in task difficulty. The literature offers two potentially complimentary interpretations of the role of the insula in future simulation that are commensurate with our data. First, the insula has been shown to be integral to the detection and processing of salient information (Menon & Uddin, 2010; Uddin, 2015). This function is not restricted to a particular modality, applicable to “odd-ball” targets in both visual and auditory domains (e.g. Linden et al., 1999). Particularly relevant to the current study are a large number of studies showing, across a range of cognitive domains, that the insula is sensitive to experimental paradigms involving the matching of unexpected or incongruent stimuli. For example, Meyer, Greenlee & Wuerger (2011) have shown greater activation in the left anterior insula for incongruent audio-visual pairings (body movements and speech sounds) relative to congruent pairings. Likewise, a number of studies have shown insula involvement in the processing of incongruent word-color combinations during the Stroop task (e.g. Chen, Lei, Ding, Li, & Chen, 2013; van Veen & Carter, 2005), semantically incongruent word-pairs (van der Heiden et al., 2014) and the atypical stressing of syllables during speech perception (Rothermich & Kotz, 2013). Recently, Wakusawa et al. (2015) reported insula activation when imagining using novel tools, or using familiar tools in novel situations. Together, these studies suggest a domain-general function of insula processing that involves the detection of salient stimuli that deviate from sensory, perceptual or conceptual expectations. According to this framework, the left insula effect we report in the task-PLS analysis, in which the *Incongruent* condition resulted in greater activity than the *Congruent* condition, likely reflects the registering of unusual detail combinations presented in the *Incongruent* condition as salient.

Interestingly, although the *Incongruent* condition produced increased activity in the left insula, the task PLS also produced the reversed effect in the right insula later in the temporal window, with greater BOLD signal associated with the *Congruent* condition. The reason for this discrepancy in effects in left and right insulae is unclear. The right insula has previously been shown to be involved in self-attributed evaluation of task-performance (Späti et al., 2014) and, given the phenomenological differences between the two conditions (e.g. difficulty, detail, plausibility), it is possible that the right insula activity in our task corresponds to participants' evaluation of their own performance on the simulation task. This is unlikely, however, as Späti et al. (2014) showed that self-attributed poor performance was associated with *increased* activity in the right insula, while in the current study the condition on which participants would have likely judged their performance as poor (i.e. the *Incongruent* condition) produced *decreased* activity. Resting-state functional connectivity studies have shown lateralized connectivity effects in the insula (Cauda et al., 2011; Sridharan, Levitin, & Menon, 2008), and further research is required to investigate how such lateralized functions are related to episodic simulation, as suggested by the current study.

In addition to registering unexpected or incongruent stimuli, as a key node of the SN, a second key function of the insula is the initiation of the switch between activation of the DMN and FPCN (Menon & Uddin, 2010; Uddin, 2015). Furthermore, recent work has implicated the anterior insula in the dynamic coupling of these networks during creative tasks that require cognitive flexibility (e.g., divergent thinking tasks; Beaty et al., 2015, 2016), with DMN regions initially showing connectivity with the insula early on in the task, before coupling with regions in the FPCN. Similarly, our ws-seed PLS results show that the trial-to-trial variability in the magnitude of the BOLD response in certain DMN regions is associated with the degree of deactivation in the left insula: those trials in which the angular gyrus and temporal pole respond maximally to the *Incongruent* condition are accompanied by the left insula "staying online", but during trials when these regions are weakly engaged, the insula is strongly deactivated. During the *Congruent* condition, however, the left insula shows enhanced functional connectivity with regions in the FPCN and SN. These functional connectivity findings are interesting because, while previous research has focused on the SN's role in switching between networks in response to externally-directed tasks that typically result in the suppression of the DMN (Sridharan, Levitin, & Menon, 2008; Uddin, 2015), our findings suggest that the left insula is also capable of increasing DMN activity when required during "salient internal thought" (Andrews-Hanna, Smallwood, & Spreng, 2014).

To summarize, our findings suggest that the left insula plays an important role in both registering unusual memory detail sets as salient, as well as coupling with DMN regions to enable successful construction of imagined future events involving incongruent memory details. However, it should be noted that previous research has implicated an additional mechanism responsible for the switching between networks during autobiographical thinking: Spreng, Stevens, Chamberlain, Gilmore, & Schacter (2010) found that it was the FPCN that flexibly switches from being coupled with the DMN and (in that study) the dorsal attention network depending on current task demands. However, although their task was autobiographical, it required participants to engage in long-term planning rather than to construct future simulations. Thus, taken together with our findings, it would appear that the

mechanisms associated with changes in network coupling vary depending on specific experimental contexts and forms of autobiographical thinking.

Motivated by previous behavioral work highlighting the relationship between episodic future simulation and divergent thinking (Addis et al., 2016; Madore, Addis, & Schacter, 2015; Madore, Jing, & Schacter, 2016), we explored whether our behavioral and BOLD variables were associated with this form of cognitive flexibility (as measured by the AUT flexibility scores). Our results revealed that AUT flexibility scores were negatively correlated with *Congruent-Incongruent* difference scores for both plausibility and difficulty ratings. This finding suggests that more flexible individuals are less affected by the increasing recombinatory demands associated with the *Incongruent* condition, providing further behavioral evidence for the link between divergent thinking and episodic simulation. Additionally, our behavior PLS analysis showed that brain activation during both conditions was linearly associated with AUT flexibility scores in a number of DMN and FPCN regions. Specifically, clusters in bilateral rostrolateral prefrontal cortices (extending into both the DMN and FPCN) showed positive correlations with flexibility scores, demonstrating that cognitively flexible individuals recruit these regions during future imagination to a greater degree than less cognitively flexible individuals. Rostrolateral prefrontal cortex has been associated with a diverse range of cognitive domains, including mentalizing, episodic retrieval and working memory (Gilbert et al., 2006), suggesting that it carries out domain-general processes (Wendelken, Chung, & Bunge, 2012). A large body of research has also implicated the rostrolateral prefrontal cortex in relational integration, reasoning, and the evaluation of self-generated thought (Christoff et al., 2001; Ellamil et al., 2012; Green, Kraemer, Fugelsang, Gray, & Dunbar, 2010; Wendelken & Bunge, 2009; Wendelken et al., 2012; Wendelken, Nakhabenko, Donohue, Carter, & Bunge, 2007; Westphal, Reggente, Ito, & Rissman, 2016). Thus, we propose that when completing an episodic simulation task in which participants are provided with specific details to integrate together, the rostrolateral prefrontal cortex may support the generation and evaluation of *reasons* for the co-occurrence of episodic details that have not occurred together in the past – and that cognitively flexible individuals recruit this region to a greater degree, thereby providing a more plausible context for their imagined scenario. This form of relational reasoning relies not merely on the retrieval of episodic memories but also on semantic information (e.g., schemas), thereby providing a plausible “semantic scaffolding” to guide the simulation of a novel yet coherent event (Irish et al., 2012; Irish & Piguet, 2013).

Indeed, the behavior PLS analysis also showed that activity in the right lateral temporal pole —a region strongly associated with the representation of semantic information (Bonner & Price, 2013; Lambon Ralph, Pobric, & Jefferies, 2009; Lambon Ralph, Sage, Jones, & Mayberry, 2010) , including autobiographical semantic information (Graham, Lee, Brett, & Patterson, 2003)—was also positively correlated with cognitive flexibility. Interestingly, anterior temporal regions also showed increased functional connectivity to the left insula during the *Incongruent* condition. In addition, the right angular gyrus, which has been shown to exhibit greater coupling with medial temporal lobe regions during autobiographical memory retrieval relative to rest (Bellana, Liu, Anderson, Moscovitch, & Grady, 2016), and has been linked with semantic processing (Binder et al., 2009; Price, Bonner, Peelle, & Grossman, 2015; Seghier, 2013), also exhibited preferential connectivity to the insula during

the *Incongruent* condition. Together these results suggest that, in addition to more flexible recruitment of semantic regions during future imagination, decreasing the congruence of memory details comprising an imagined event is associated with increased coupling of the insula to DMN regions mediating semantic processing.

Although activity in the rostrolateral prefrontal and temporopolar cortices was positively correlated with AUT flexibility scores during simulation, there were also a number of regions that exhibited negative relationships with cognitive flexibility. Most surprising of these regions was the left hippocampus—a region previously implicated in both future simulation (Addis & Schacter, 2012; Benoit & Schacter, 2015) and flexible, creative thinking (Duff, Kurczek, Rubin, Cohen, & Tranel, 2013; Ellamil et al., 2012; Rubin, Watson, Duff, & Cohen, 2014). Given that rostrolateral prefrontal cortex and the hippocampus are both involved in relational processing (Wendelken & Bunge, 2009), it is possible that one's individual level of cognitive flexibility influences the strategy adopted during the task. Specifically, it may be that individuals with lower cognitive flexibility engage the hippocampus to form more concrete, contextual relations between disparate episodic details while highly flexible individuals link episodic details in a meaningful way by engaging in higher-level autobiographical reasoning, via operations in the rostrolateral prefrontal and temporopolar cortices, to generate a framework in which novel scenarios can occur.

Another possibility is that the negative association between left hippocampal activity and AUT flexibility scores is due to highly flexible individuals being able to inhibit the *automatic*, hippocampally-mediated retrieval of episodic details (i.e., pattern completion) during the construction of future events, and instead restrict retrieval to only those details consistent with task demands. Indeed, it has been shown that one of the key components to generating novel responses in the AUT is the ability to inhibit the activation of memory details directly associated with a cue, thereby avoiding obvious responses (Beaty & Silvia, 2012). According to Beaty and Silvia, the automatic retrieval of memories and concepts directly related to the AUT cue interferes with the ability to generate novel and creative responses. Thus, with respect to the current study, it could be the case that the automatic retrieval of details directly related to the cues in the recombination paradigm interferes with the generation of novel scenarios. One feature of the current data that supports this proposal is that the relationship between AUT flexibility scores and simulation-related activity in the left HC evident in the behavioural PLS was driven by the *Congruent* condition ($r = -.577$, $p = .005$) when the automatic retrieval of episodic details is likely greater (given the provided detail are related), while this relationship was not significant for the *Incongruent* condition ($r = -.225$, $p = .314$).

In addition to a negative relationship with the left hippocampus, AUT flexibility scores were also negatively correlated with bilateral ventrolateral prefrontal cortices and amygdalae. We have previously reported amygdala activation when employing versions of this recombination paradigm (Addis, Pan, et al., 2009; Martin et al., 2011), and have attributed this activity to novelty processing related to unusual detail sets (van Mulukom et al., 2013) . The finding that this novelty signal is negatively correlated with cognitive flexibility suggests that more flexible individuals experience these simulations as less unusual or bizarre. This interpretation is supported by the finding that increasing divergent thinking

ability was associated with smaller differences in plausibility ratings between *Congruent* and *Incongruent* conditions – a result that indicates that more flexible individuals rated the future events they constructed from incongruent details as more similar in plausibility to the future events based on congruent details.

While episodic future simulation has generally been regarded as a process subserved by increased activation in the core network/ DMN, we have used multivariate analysis techniques to show that increasing the relational demands associated with future imagination results in reduced recruitment of key DMN nodes, increased activation in areas within the SN and increased functional connectivity between SN and DMN regions. In addition, individual differences in cognitive flexibility covary with engagement of regions in both the FPCN and DMN during episodic simulation, highlighting the complex interaction of these networks during forms of flexible cognition (Beaty et al., 2015, 2016; Ellamil et al., 2012; Spreng et al., 2010), including imagination of personal future scenarios.

Supplementary Material

Refer to Web version on PubMed Central for supplementary material.

Acknowledgments

This work was supported by a Marsden Fund grant (12-UOA-254) and Rutherford Discovery Fellowship (RDF-10-UOA-024) awarded to DRA. DLS was supported by NIMH grant MH060941. We thank Inge Strauss and Jae-Min Lee for scoring of Alternate Uses Task responses, and Carolin Wickner for data collation.

References

Abraham A, Schubotz RI, von Cramon DY. Thinking about the future versus the past in personal and non-personal contexts. Brain Research. 2008; 1233:106–119. http://doi.org/10.1016/j.brainres.2008.07.084. [PubMed: 18703030]

Addis, DR., Cheng, T., Roberts, RP., Schacter, DL. Hippocampal contributions to the episodic simulation of specific and general future events. Hippocampus. 2010. http://doi.org/10.1002/hipo.20870

Addis DR, McIntosh AR, Moscovitch M, Crawley AP, McAndrews MP. Characterizing spatial and temporal features of autobiographical memory retrieval networks: a partial least squares approach. NeuroImage. 2004; 23(4):1460–1471. http://doi.org/10.1016/j.neuroimage.2004.08.007. [PubMed: 15589110]

Addis DR, Pan L, Musicaro R, Schacter DL. Divergent thinking and constructing episodic simulations. Memory (Hove, England). 2016; 24(1):89–97. http://doi.org/10.1080/09658211.2014.985591.

Addis DR, Pan L, Vu M-A, Laiser N, Schacter DL. Constructive episodic simulation of the future and the past: distinct subsystems of a core brain network mediate imagining and remembering. Neuropsychologia. 2009; 47(11):2222–2238. http://doi.org/10.1016/j.neuropsychologia.2008.10.026. [PubMed: 19041331]

Addis DR, Roberts RP, Schacter DL. Age-related neural changes in autobiographical remembering and imagining. Neuropsychologia. 2011; 49(13):3656–3669. http://doi.org/10.1016/j.neuropsychologia.2011.09.021. [PubMed: 21945808]

Addis DR, Sacchetti DC, Ally BA, Budson AE, Schacter DL. Episodic simulation of future events is impaired in mild Alzheimer's disease. Neuropsychologia. 2009; 47(12):2660–2671. http://doi.org/10.1016/j.neuropsychologia.2009.05.018. [PubMed: 19497331]

Addis DR, Schacter DL. Effects of detail and temporal distance of past and future events on the engagement of a common neural network. Hippocampus. 2008; 18:227–237. [PubMed: 18157862]

Addis DR, Wong AT, Schacter DL. Remembering the past and imagining the future: common and distinct neural substrates during event construction and elaboration. Neuropsychologia. 2007; 45(7): 1363–1377. http://doi.org/10.1016/j.neuropsychologia.2006.10.016. [PubMed: 17126370]

Addis DR, Wong AT, Schacter DL. Age-related changes in the episodic simulation of future events. Psychological Science: A Journal of the American Psychological Society / APS. 2008; 19(1):33–41. http://doi.org/10.1111/j.1467-9280.2008.02043.x.

Andelman F, Hoofien D, Goldberg I, Aizenstein O, Neufeld MY. Bilateral hippocampal lesion and a selective impairment of the ability for mental time travel. Neurocase. 2010; 16(5):426–435. http://doi.org/10.1080/13554791003623318. [PubMed: 20401802]

Andrews-Hanna JR, Smallwood J, Spreng RN. The default network and self-generated thought: component processes, dynamic control, and clinical relevance. Annals of the New York Academy of Sciences. 2014; 1316(1):29–52. http://doi.org/10.1111/nyas.12360. [PubMed: 24502540]

Axmacher N, Henseler MM, Jensen O, Weinreich I, Elger CE, Fell J. Cross-frequency coupling supports multi-item working memory in the human hippocampus. Proceedings of the National Academy of Sciences of the United States of America. 2010; 107(7):3228–3233. http://doi.org/10.1073/pnas.0911531107. [PubMed: 20133762]

Bartlett, FC. Remembering. 1932. Retrieved March 22, 2016, from http://www.cambridge.org/nz/academic/subjects/psychology/cognition/remembering-study-experimental-and-social-psychology-2nd-edition?format=PB&isbn=9780521483568

Bastin, J., Deman, P., David, O., Gueguen, M., Benis, D., Minotti, L., Jerbi, K. Direct recordings from human anterior insula reveal its leading role within the error-monitoring network. Cerebral Cortex. 2016. bhv352http://doi.org/10.1093/cercor/bhv352

Beaty RE, Benedek M, Kaufman SB, Silvia PJ. Default and executive network coupling supports creative idea production. Scientific Reports. 2015; 5:10964. http://doi.org/10.1038/srep10964. [PubMed: 26084037]

Beaty RE, Benedek M, Silvia PJ, Schacter DL. Creative Cognition and Brain Network Dynamics. Trends in Cognitive Sciences. 2016; 20(2):87–95. http://doi.org/10.1016/j.tics.2015.10.004. [PubMed: 26553223]

Beaty RE, Silvia PJ. Why do ideas get more creative across time? An executive interpretation of the serial order effect in divergent thinking tasks. Psychology of Aesthetics, Creativity, and the Arts. 2012; 6(4):309–319. http://doi.org/10.1037/a0029171.

Beaty RE, Silvia PJ, Nusbaum EC, Jauk E, Benedek M. The roles of associative and executive processes in creative cognition. Memory & Cognition. 2014; 42(7):1186–1197. http://doi.org/10.3758/s13421-014-0428-8. [PubMed: 24898118]

Bellana B, Liu Z, Anderson JA, Moscovitch M, Grady CL. Laterality effects in functional connectivity of the angular gyrus during rest and episodic retrieval. Neuropsychologia. 2016; 80:24–34. [PubMed: 26559474]

Benedek M, Jauk E, Fink A, Koschutnig K, Reishofer G, Ebner F, Neubauer AC. To create or to recall? Neural mechanisms underlying the generation of creative new ideas. NeuroImage. 2014; 88:125–133. http://doi.org/10.1016/j.neuroimage.2013.11.021. [PubMed: 24269573]

Benedek M, Jauk E, Sommer M, Arendasy M, Neubauer AC. Intelligence, creativity, and cognitive control: The common and differential involvement of executive functions in intelligence and creativity. Intelligence. 2014; 46:73–83. http://doi.org/10.1016/j.intell.2014.05.007. [PubMed: 25278640]

Benoit RG, Schacter DL. Specifying the core network supporting episodic simulation and episodic memory by activation likelihood estimation. Neuropsychologia. 2015; 75:450–457. http://doi.org/10.1016/j.neuropsychologia.2015.06.034. [PubMed: 26142352]

Binder JR, Desai RH. The neurobiology of semantic memory. Trends in Cognitive Sciences. 2011; 15(11):527–536. http://doi.org/10.1016/j.tics.2011.10.001. [PubMed: 22001867]

Binder JR, Desai RH, Graves WW, Conant LL. Where Is the semantic system? A critical review and meta-Analysis of 120 functional neuroimaging studies. Cerebral Cortex. 2009; 19(12):2767–2796. http://doi.org/10.1093/cercor/bhp055. [PubMed: 19329570]

Bonner MF, Price AR. Where is the anterior temporal lobe and what does it do? The Journal of Neuroscience. 2013; 33(10):4213–4215. http://doi.org/10.1523/JNEUROSCI.0041-13.2013. [PubMed: 23467339]

Buckner RL, Carroll DC. Self-projection and the brain. Trends in Cognitive Sciences. 2007; 11(2):49–57. http://doi.org/10.1016/j.tics.2006.11.004. [PubMed: 17188554]

Burianova H, Grady CL. Common and unique neural activations in autobiographical, episodic, and semantic retrieval. Journal of Cognitive Neuroscience. 2007; 19(9):1520–1534. http://doi.org/10.1162/jocn.2007.19.9.1520. [PubMed: 17714013]

Burianova H, McIntosh AR, Grady CL. A common functional brain network for autobiographical, episodic, and semantic memory retrieval. NeuroImage. 2010; 49(1):865–874. http://doi.org/10.1016/j.neuroimage.2009.08.066. [PubMed: 19744566]

Cauda F, D'Agata F, Sacco K, Duca S, Geminiani G, Vercelli A. Functional connectivity of the insula in the resting brain. NeuroImage. 2011; 55(1):8–23. http://doi.org/10.1016/j.neuroimage.2010.11.049. [PubMed: 21111053]

Chen Z, Lei X, Ding C, Li H, Chen A. The neural mechanisms of semantic and response conflicts: An fMRI study of practice-related effects in the Stroop task. NeuroImage. 2013; 66:577–584. http://doi.org/10.1016/j.neuroimage.2012.10.028. [PubMed: 23103691]

Christoff K, Prabhakaran V, Dorfman J, Zhao Z, Kroger JK, Holyoak KJ, Gabrieli JDE. Rostrolateral prefrontal cortex involvement in relational integration during deasoning. NeuroImage. 2001; 14(5):1136–1149. http://doi.org/10.1006/nimg.2001.0922. [PubMed: 11697945]

Clark JM, Paivio A. Extensions of the Paivio, Yuille, and Madigan (1968) norms. Behavior Research Methods, Instruments, & Computers: A Journal of the Psychonomic Society, Inc. 2004; 36(3):371–383.

Cole MW, Reynolds JR, Power JD, Repovs G, Anticevic A, Braver TS. Multi-task connectivity reveals flexible hubs for adaptive task control. Nature Neuroscience. 2013; 16(9):1348–1355. http://doi.org/10.1038/nn.3470. [PubMed: 23892552]

Dale AM. Optimal experimental design for event-related fMRI. Human Brain Mapping. 1999; 8(2–3):109–114. [PubMed: 10524601]

Damasio AR. Time-locked multiregional retroactivation: a systems-level proposal for the neural substrates of recall and recognition. Cognition. 1989; 33(1–2):25–62. [PubMed: 2691184]

Desikan RS, Ségonne F, Fischl B, Quinn BT, Dickerson BC, Blacker D, Killiany RJ. An automated labeling system for subdividing the human cerebral cortex on MRI scans into gyral based regions of interest. NeuroImage. 2006; 31(3):968–980. http://doi.org/10.1016/j.neuroimage.2006.01.021. [PubMed: 16530430]

Dietrich A. The cognitive neuroscience of creativity. Psychonomic Bulletin & Review. 2004; 11(6):1011–1026. http://doi.org/10.3758/BF03196731. [PubMed: 15875970]

Dubois J, Adolphs R. Building a science of individual differences from fMRI. Trends in Cognitive Sciences. 2016; 20(6):425–443. http://doi.org/10.1016/j.tics.2016.03.014. [PubMed: 27138646]

Duval C, Desgranges B, de La Sayette V, Belliard S, Eustache F, Piolino P. What happens to personal identity when semantic knowledge degrades? A study of the self and autobiographical memory in semantic dementia. Neuropsychologia. 2012; 50:254–265. http://doi:10.1016/j.neuropsychologia.2011.11.019. [PubMed: 22155259]

Duff MC, Kurczek J, Rubin R, Cohen NJ, Tranel D. Hippocampal amnesia disrupts creative thinking. Hippocampus. 2013; 23(12):1143–1149. http://doi.org/10.1002/hipo.22208. [PubMed: 24123555]

Eckert MA, Menon V, Walczak A, Ahlstrom J, Denslow S, Horwitz A, Dubno JR. At the heart of the ventral attention system: The right anterior insula. Human Brain Mapping. 2009; 30(8):2530–2541. http://doi.org/10.1002/hbm.20688. [PubMed: 19072895]

Eichenbaum H. The hippocampus and declarative memory: cognitive mechanisms and neural codes. Behavioural Brain Research. 2001; 127(1–2):199–207. http://doi.org/10.1016/S0166-4328(01)00365-5. [PubMed: 11718892]

Ellamil M, Dobson C, Beeman M, Christoff K. Evaluative and generative modes of thought during the creative process. NeuroImage. 2012; 59(2):1783–1794. http://doi.org/10.1016/j.neuroimage.2011.08.008. [PubMed: 21854855]

Eslinger PJ, Grattan LM. Frontal lobe and frontal-striatal substrates for different forms of human cognitive flexibility. Neuropsychologia. 1993; 31(1):17–28. http://doi.org/10.1016/0028-3932(93)90077-D. [PubMed: 8437679]

Fonov V, Evans AC, Botteron K, Almli CR, McKinstry RC, Collins DL. Unbiased average age-appropriate atlases for pediatric studies. NeuroImage. 2011; 54(1):313–327. http://doi.org/10.1016/j.neuroimage.2010.07.033. [PubMed: 20656036]

Gaesser B, Spreng RN, McLelland VC, Addis DR, Schacter DL. Imagining the future: Evidence for a hippocampal contribution to constructive processing. Hippocampus. 2013; 23(12):1150–1161. http://doi.org/10.1002/hipo.22152. [PubMed: 23749314]

Geisser S, Greenhouse SW. An extension of Box's results on the use of the F distribution in multivariate analysis. The Annals of Mathematical Statistics. 1958; 29(3):885–891.

Gilbert DT, Wilson TD. Prospection: Experiencing the future. Science. 2007; 317(5843):1351–1354. http://doi.org/10.1126/science.1144161. [PubMed: 17823345]

Gilbert SJ, Spengler S, Simons JS, Steele JD, Lawrie SM, Frith CD, Burgess PW. Functional specialization within rostral prefrontal cortex (area 10): a meta-analysis. Journal of Cognitive Neuroscience. 2006; 18(6):932–948. http://doi.org/10.1162/jocn.2006.18.6.932. [PubMed: 16839301]

Gilhooly KJ, Fioratou E, Anthony SH, Wynn V. Divergent thinking: Strategies and executive involvement in generating novel uses for familiar objects. British Journal of Psychology. 2007; 98(4):611–625. http://doi.org/10.1111/j.2044-8295.2007.tb00467.x. [PubMed: 17535464]

Gilmore AW, Nelson SM, McDermott KB. The contextual association network activates more for remembered than for imagined events. Cerebral Cortex. 2016; 26(2):611–617. http://doi.org/10.1093/cercor/bhu223. [PubMed: 25260708]

Graham KS, Lee ACH, Brett M, Patterson K. The neural basis of autobiographical and semantic memory: new evidence from three PET studies. Cognitive, Affective, & Behavioral Neuroscience. 2003; 3(3):234–254.

Green AE, Kraemer DJM, Fugelsang JA, Gray JR, Dunbar KN. Connecting long distance: Semantic distance in analogical reasoning modulates frontopolar cortex activity. Cerebral Cortex. 2010; 20(1):70–76. http://doi.org/10.1093/cercor/bhp081. [PubMed: 19383937]

Guilford, JP. The nature of human intelligence. McGraw-Hill; 1967.

Hannula DE, Ranganath C. Medial temporal lobe activity predicts successful relational memory binding. The Journal of Neuroscience. 2008; 28(1):116–124. http://doi.org/10.1523/JNEUROSCI.3086-07.2008. [PubMed: 18171929]

Hannula DE, Tranel D, Cohen NJ. The long and the short of it: Relational memory impairments in amnesia, even at short lags. The Journal of Neuroscience. 2006; 26(32):8352–8359. http://doi.org/10.1523/JNEUROSCI.5222-05.2006. [PubMed: 16899730]

Hassabis D, Kumaran D, Vann SD, Maguire EA. Patients with hippocampal amnesia cannot imagine new experiences. Proceedings of the National Academy of Sciences of the United States of America. 2007; 104(5):1726–1731. http://doi.org/10.1073/pnas.0610561104. [PubMed: 17229836]

Hirshhorn M, Grady C, Rosenbaum RS, Winocur G, Moscovitch M. Brain regions involved in the retrieval of spatial and episodic details associated with a familiar environment: An fMRI study. Neuropsychologia. 2012; 50(13):3094–3106. http://doi.org/10.1016/j.neuropsychologia.2012.08.008. [PubMed: 22910274]

Hutton C, Bork A, Josephs O, Deichmann R, Ashburner J, Turner R. Image distortion correction in fMRI: A quantitative evaluation. NeuroImage. 2002; 16(1):217–240. http://doi.org/10.1006/nimg.2001.1054. [PubMed: 11969330]

Irish M, Addis DR, Hodges JR, Piguet O. Considering the role of semantic memory in episodic future thinking: evidence from semantic dementia. Brain. 2012; 135(7):2178–2191. http://doi.org/10.1093/brain/aws119. [PubMed: 22614246]

Irish M, Piguet O. The pivotal role of semantic memory in remembering the past and imagining the future. Frontiers in Behavioral Neuroscience. 2013; 7 http://doi.org/10.3389/fnbeh.2013.00027.

Klein SB, Loftus J, Kihlstrom JF. Memory and temporal experience: The effects of episodic memory loss on an amnesic patient's ability to remember the past and imagine the future. Social Cognition. 20(5):353–379. n.d.

Kosillo P, Smith AT. The role of the human anterior insular cortex in time processing. Brain Structure and Function. 2010; 214(5–6):623–628. http://doi.org/10.1007/s00429-010-0267-8. [PubMed: 20512365]

Kwan D, Carson N, Addis DR, Rosenbaum RS. Deficits in past remembering extend to future imagining in a case of developmental amnesia. Neuropsychologia. 2010; 48(11):3179–3186. http://doi.org/10.1016/j.neuropsychologia.2010.06.011. [PubMed: 20561535]

Lambon Ralph MA, Pobric G, Jefferies E. Conceptual knowledge is underpinned by the temporal pole bilaterally: convergent evidence from rTMS. Cerebral Cortex (New York, N.Y.: 1991). 2009; 19(4):832–838. http://doi.org/10.1093/cercor/bhn131.

Lambon Ralph MA, Sage K, Jones RW, Mayberry EJ. Coherent concepts are computed in the anterior temporal lobes. Proceedings of the National Academy of Sciences of the United States of America. 2010; 107(6):2717–2722. http://doi.org/10.1073/pnas.0907307107. [PubMed: 20133780]

Linden DE, Prvulovic D, Formisano E, Völlinger M, Zanella FE, Goebel R, Dierks T. The functional neuroanatomy of target detection: an fMRI study of visual and auditory oddball tasks. Cerebral Cortex (New York, N.Y.: 1991). 1999; 9(8):815–823.

Mace JH. Involuntary autobiographical memory chains: Implications for autobiographical memory organization. Frontiers in Psychiatry. 2014; 5 http://doi.org/10.3389/fpsyt.2014.00183.

Madore KP, Addis DR, Schacter DL. Creativity and memory: Effects of an episodic-specificity induction on divergent thinking. Psychological Science. 2015; 26(9):1461–1468. http://doi.org/10.1177/0956797615591863. [PubMed: 26205963]

Madore KP, Jing HG, Schacter DL. Divergent creative thinking in young and older adults: Extending the effects of an episodic specificity induction. Memory & Cognition. 2016; 44:974–988. [PubMed: 27001170]

Madore KP, Szpunar KK, Addis DR, Schacter DL. Episodic specifcity induction impacts activity in a core brain network during construction of imagined future experiences. Proceedings of the National Academy of Sciences USA. 2016; 113:10696–10701. http://doi/10.1073/pnas.1612278113.

Martin VC, Schacter DL, Corballis MC, Addis DR. A role for the hippocampus in encoding simulations of future events. Proceedings of the National Academy of Sciences. 2011; 108:13858–13863. http://doi.org/10.1073/pnas.1105816108.

McClelland JL, McNaughton BL, O'Reilly RC. Why there are complementary learning systems in the hippocampus and neocortex: insights from the successes and failures of connectionist models of learning and memory. Psychological Review. 1995; 102(3):419–457. [PubMed: 7624455]

McIntosh AR, Bookstein FL, Haxby JV, Grady CL. Spatial pattern analysis of functional brain images using partial least squares. NeuroImage. 1996; 3(3 Pt 1):143–157. http://doi.org/10.1006/nimg.1996.0016. [PubMed: 9345485]

Menon V, Uddin LQ. Saliency, switching, attention and control: a network model of insula function. Brain Structure & Function. 2010; 214(5–6):655–667. http://doi.org/10.1007/s00429-010-0262-0. [PubMed: 20512370]

Meyer GF, Greenlee M, Wuerger S. Interactions between auditory and visual semantic stimulus classes: Evidence for common processing networks for speech and body actions. Journal of Cognitive Neuroscience. 2011; 23(9):2291–2308. http://doi.org/10.1162/jocn.2010.21593. [PubMed: 20954938]

Niendam TA, Laird AR, Ray KL, Dean YM, Glahn DC, Carter CS. Meta-analytic evidence for a superordinate cognitive control network subserving diverse executive functions. Cognitive, Affective & Behavioral Neuroscience. 2012; 12(2):241–268. http://doi.org/10.3758/s13415-011-0083-5.

Norman KA, O'Reilly RC. Modeling hippocampal and neocortical contributions to recognition memory: a complementary-learning-systems approach. Psychological Review. 2003; 110(4):611–646. http://doi.org/10.1037/0033-295X.110.4.611. [PubMed: 14599236]

Oldfield RC. The assessment and analysis of handedness: the Edinburgh inventory. Neuropsychologia. 1971; 9(1):97–113. [PubMed: 5146491]

Price AR, Bonner MF, Peelle JE, Grossman M. Converging Evidence for the Neuroanatomic Basis of Combinatorial Semantics in the Angular Gyrus. The Journal of Neuroscience. 2015; 35(7):3276–3284. http://doi.org/10.1523/JNEUROSCI.3446-14.2015. [PubMed: 25698762]

Race E, Keane MM, Verfaellie M. Losing sight of the future: Impaired semantic prospection following medial temporal lobe lesions. Hippocampus. 2013; 23(4):268–277. http://doi.org/10.1002/hipo.22084. [PubMed: 23197413]

Rissman J, Gazzaley A, D'Esposito M. Measuring functional connectivity during distinct stages of a cognitive task. NeuroImage. 2004; 23(2):752–763. http://doi.org/10.1016/j.neuroimage.2004.06.035. [PubMed: 15488425]

Roberts, RP., Hach, S., Tippett, LJ., Addis, DR. The Simpson's paradox and fMRI: Similarities and differences between functional connectivity measures derived from within-subject and across-subject correlations. NeuroImage. 2016. http://doi.org/10.1016/j.neuroimage.2016.04.028

Rothermich K, Kotz SA. Predictions in speech comprehension: fMRI evidence on the meter-semantic interface. NeuroImage. 2013; 70:89–100. http://doi.org/10.1016/j.neuroimage.2012.12.013. [PubMed: 23291188]

Rubin, RD., Watson, PD., Duff, MC., Cohen, NJ. The role of the hippocampus in flexible cognition and social behavior; Frontiers in Human Neuroscience. 2014. p. 8http://doi.org/10.3389/fnhum.2014.00742

Schacter DL. Adaptive constructive processes and the future of memory. The American Psychologist. 2012; 67(8):603–613. http://doi.org/10.1037/a0029869. [PubMed: 23163437]

Schacter DL, Addis DR. The cognitive neuroscience of constructive memory: remembering the past and imagining the future. Philosophical Transactions of the Royal Society of London. Series B, Biological Sciences. 2007; 362(1481):773–786. http://doi.org/10.1098/rstb.2007.2087. [PubMed: 17395575]

Schacter DL, Addis DR, Buckner RL. Remembering the past to imagine the future: the prospective brain. Nature Reviews. Neuroscience. 2007; 8(9):657–661. http://doi.org/10.1038/nrn2213. [PubMed: 17700624]

Schacter DL, Addis DR, Hassabis D, Martin VC, Spreng RN, Szpunar KK. The Future of Memory: Remembering, Imagining, and the Brain. Neuron. 2012; 76(4) http://doi.org/10.1016/j.neuron.2012.11.001.

Schacter, DL., Addis, DR., Szpunar, KK. Escaping the past: Contributions of the hippocampus to future thinking and imagination. In: Hannula, DE., Duff, MC., editors. The Hippocampus from Cells to Systems: Structure, Connectivity, and Functional Contributions to Memory and Flexible Cognition. New York: Springer; in press

Schacter DL, Norman KA, Koutstaal W. The cognitive neuroscience of constructive memory. Annual Review of Psychology. 1998; 49:289–318. http://doi.org/10.1146/annurev.psych.49.1.289.

Seghier ML. The angular gyrus: Multiple functions and multiple subdivisions. The Neuroscientist. 2013; 19(1):43–61. http://doi.org/10.1177/1073858412440596. [PubMed: 22547530]

Späti J, Chumbley J, Brakowski J, Dörig N, Grosse Holtforth M, Seifritz E, Spinelli S. Functional lateralization of the anterior insula during feedback processing. Human Brain Mapping. 2014; 35(9):4428–4439. http://doi.org/10.1002/hbm.22484. [PubMed: 24753396]

Spreng RN, Grady CL. Patterns of brain activity supporting autobiographical memory, prospection, and theory of mind, and their relationship to the default mode network. Journal of Cognitive Neuroscience. 2010; 22(6):1112–1123. [PubMed: 19580387]

Spreng RN, Stevens WD, Chamberlain JP, Gilmore AW, Schacter DL. Default network activity, coupled with the frontoparietal control network, supports goal-directed cognition. NeuroImage. 2010; 53(1):303–317. http://doi.org/10.1016/j.neuroimage.2010.06.016. [PubMed: 20600998]

Squire LR. Memory and the hippocampus: a synthesis from findings with rats, monkeys, and humans. Psychological Review. 1992; 99(2):195–231. [PubMed: 1594723]

Squire LR, van der Horst AS, McDuff SGR, Frascino JC, Hopkins RO, Mauldin KN. Role of the hippocampus in remembering the past and imagining the future. Proceedings of the National Academy of Sciences of the United States of America. 2010; 107(44):19044–19048. http://doi.org/10.1073/pnas.1014391107. [PubMed: 20956323]

Sridharan D, Levitin DJ, Menon V. A critical role for the right fronto-insular cortex in switching between central-executive and default-mode networks. Proceedings of the National Academy of Sciences. 2008; 105(34):12569–12574. http://doi.org/10.1073/pnas.0800005105.

Staresina BP, Davachi L. Mind the gap: Binding experiences across space and time in the human hippocampus. Neuron. 2009; 63(2):267–276. http://doi.org/10.1016/j.neuron.2009.06.024. [PubMed: 19640484]

Suddendorf T, Corballis MC. The evolution of foresight: What is mental time travel, and is it unique to humans? The Behavioral and Brain Sciences. 2007; 30(3) 299-313-351 http://doi.org/10.1017/S0140525×07001975.

Szpunar KK, Spreng RN, Schacter DL. A taxonomy of prospection: Introducing an organizational framework for future-oriented cognition: Fig. 1. Proceedings of the National Academy of Sciences. 2014; 111(52):18414–18421. http://doi.org/10.1073/pnas.1417144111.

Szpunar KK, Watson JM, McDermott KB. Neural substrates of envisioning the future. Proceedings of the National Academy of Sciences of the United States of America. 2007; 104(2):642–647. http://doi.org/10.1073/pnas.0610082104. [PubMed: 17202254]

Takeuchi H, Taki Y, Hashizume H, Sassa Y, Nagase T, Nouchi R, Kawashima R. Failing to deactivate: The association between brain activity during a working memory task and creativity. NeuroImage. 2011; 55(2):681–687. http://doi.org/10.1016/j.neuroimage.2010.11.052. [PubMed: 21111830]

Taylor SF, Stern ER, Gehring WJ. Neural systems for error monitoring recent findings and theoretical perspectives. The Neuroscientist. 2007; 13(2):160–172. http://doi.org/10.1177/1073858406298184. [PubMed: 17404376]

Tomer R, Fisher T, Giladi N, Aharon-Peretz J. Dissociation between spontaneous and reactive flexibility in early Parkinson's disease. Neuropsychiatry, Neuropsychology, and Behavioral Neurology. 2002; 15(2):106–112.

Tregellas JR, Davalos DB, Rojas DC. Effect of task difficulty on the functional anatomy of temporal processing. NeuroImage. 2006; 32(1):307–315. http://doi.org/10.1016/j.neuroimage.2006.02.036. [PubMed: 16624580]

Uddin LQ. Salience processing and insular cortical function and dysfunction. Nature Reviews Neuroscience. 2015; 16(1):55–61. http://doi.org/10.1038/nrn3857.

van der Heiden L, Liberati G, Sitaram R, Kim S, Jaśkowski P, Raffone A, Veit R. Insula and inferior frontal triangularis activations distinguish between conditioned brain responses using emotional sounds for basic BCI communication. Frontiers in Behavioral Neuroscience. 2014; 8 http://doi.org/10.3389/fnbeh.2014.00247.

van Mulukom V, Schacter DL, Corballis MC, Addis DR. Re-imagining the future: repetition decreases hippocampal involvement in future simulation. PloS One. 2013; 8(7):e69596. http://doi.org/10.1371/journal.pone.0069596. [PubMed: 23936055]

van Mulukom V, Schacter DL, Corballis MC, Addis DR. The degree of disparateness of event details modulates future simulation construction, plausibility, and recall. The Quarterly Journal of Experimental Psychology. 2016; 69(2):234–242. http://doi.org/10.1080/17470218.2015.1051559. [PubMed: 26052883]

van Veen V, Carter CS. Separating semantic conflict and response conflict in the Stroop task: A functional MRI study. NeuroImage. 2005; 27(3):497–504. http://doi.org/10.1016/j.neuroimage.2005.04.042. [PubMed: 15964208]

Viard A, Chételat G, Lebreton K, Desgranges B, Landeau B, de La Sayette V, Piolino P. Mental time travel into the past and the future in healthy aged adults: an fMRI study. Brain and Cognition. 2011; 75(1):1–9. http://doi.org/10.1016/j.bandc.2010.10.009. [PubMed: 21093970]

Viard A, Piolino P, Belliard S, Sayette V, de L, Desgranges B, Eustache F. Episodic future thinking in semantic dementia: A cognitive and fMRI Study. PLOS ONE. 2014; 9(10):e111046. http://doi.org/10.1371/journal.pone.0111046. [PubMed: 25333997]

Wakusawa K, Sugiura M, Sassa Y, Jeong H, Yomogida Y, Horie K, Kawashima R. Adaptive ability to cope with atypical or novel situations involving tool use: an fMRI approach. Neuroscience Research. 2015; 90:72–82. http://doi.org/10.1016/j.neures.2014.03.008. [PubMed: 24709370]

Weiler JA, Suchan B, Daum I. Foreseeing the future: occurrence probability of imagined future events modulates hippocampal activation. Hippocampus. 2010; 20(6):685–690. http://doi.org/10.1002/hipo.20695. [PubMed: 19693779]

Wendelken C, Bunge SA. Transitive inference: Distinct contributions of rostrolateral prefrontal cortex and the hippocampus. Journal of Cognitive Neuroscience. 2009; 22(5):837–847. http://doi.org/10.1162/jocn.2009.21226.

Wendelken C, Chung D, Bunge SA. Rostrolateral prefrontal cortex: Domain-general or domain-sensitive? Human Brain Mapping. 2012; 33(8):1952–1963. http://doi.org/10.1002/hbm.21336. [PubMed: 21834102]

Wendelken C, Nakhabenko D, Donohue SE, Carter CS, Bunge SA. "Brain Is to thought as stomach Is to??": Investigating the role of rostrolateral rrefrontal cortex in relational reasoning. Journal of Cognitive Neuroscience. 2007; 20(4):682–693. http://doi.org/10.1162/jocn.2008.20055.

Westphal AJ, Reggente N, Ito KL, Rissman J. Shared and distinct contributions of rostrolateral prefrontal cortex to analogical reasoning and episodic memory retrieval. Human Brain Mapping. 2016; 37(3):896–912. http://doi.org/10.1002/hbm.23074. [PubMed: 26663572]

Wiebels, KW., Roberts, RP., Addis, DR. Controlling for behavioural confounds in partial least squares analyses; Presented at the Organization for Human Brain Mapping; Geneva, Switzerland: 2016. Retrieved from https://ww5.aievolution.com/hbm1601/index.cfm?do=abs.viewAbs&abs=2251

Yeo BTT, Krienen FM, Sepulcre J, Sabuncu MR, Lashkari D, Hollinshead M, Buckner RL. The organization of the human cerebral cortex estimated by intrinsic functional connectivity. Journal of Neurophysiology. 2011; 106(3):1125–1165. http://doi.org/10.1152/jn.00338.2011. [PubMed: 21653723]

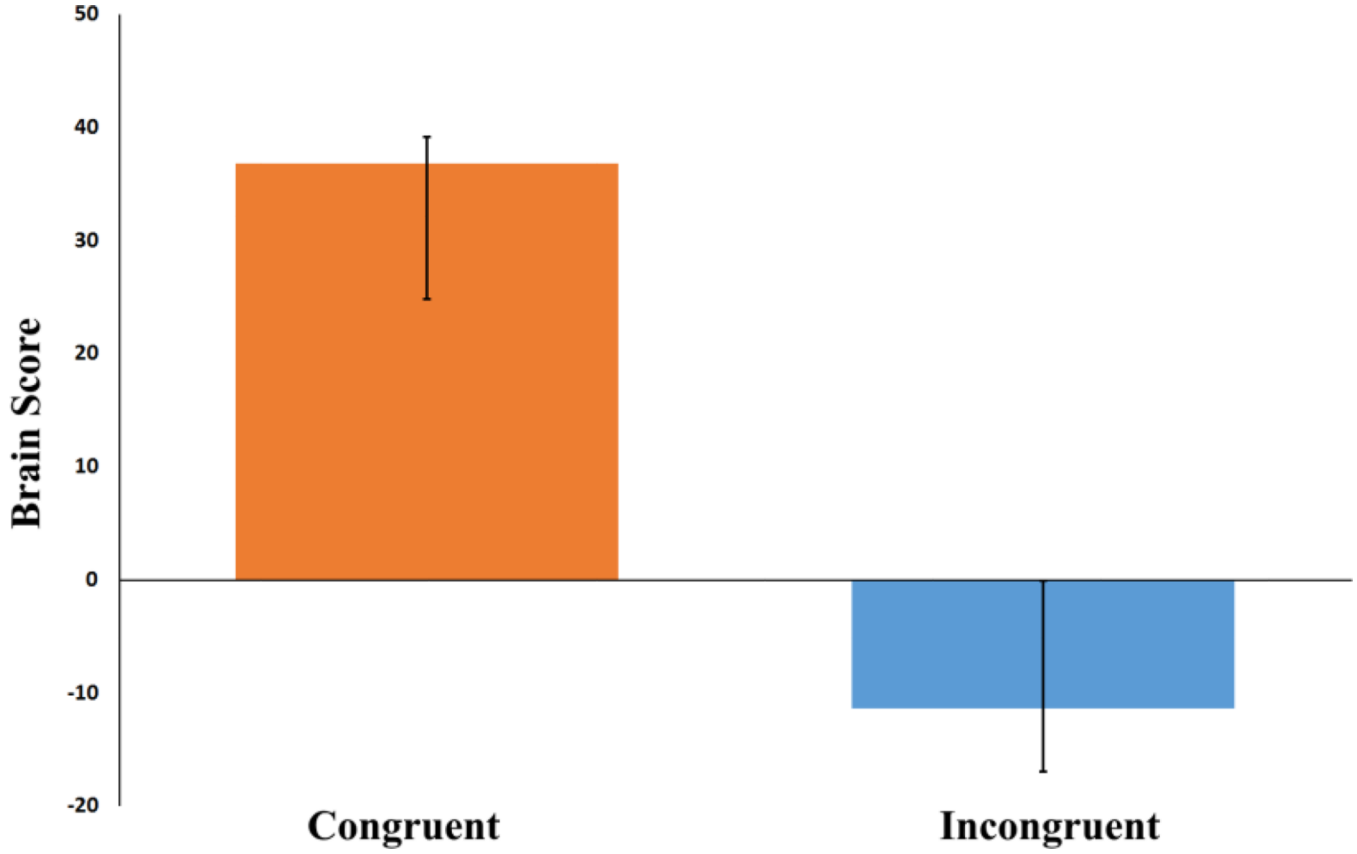

Figure 1. Average brain scores for future simulation conditions

Brain scores are weighted averages of activity across all voxels associated with each task. Error bars are bootstrapped confidence intervals.

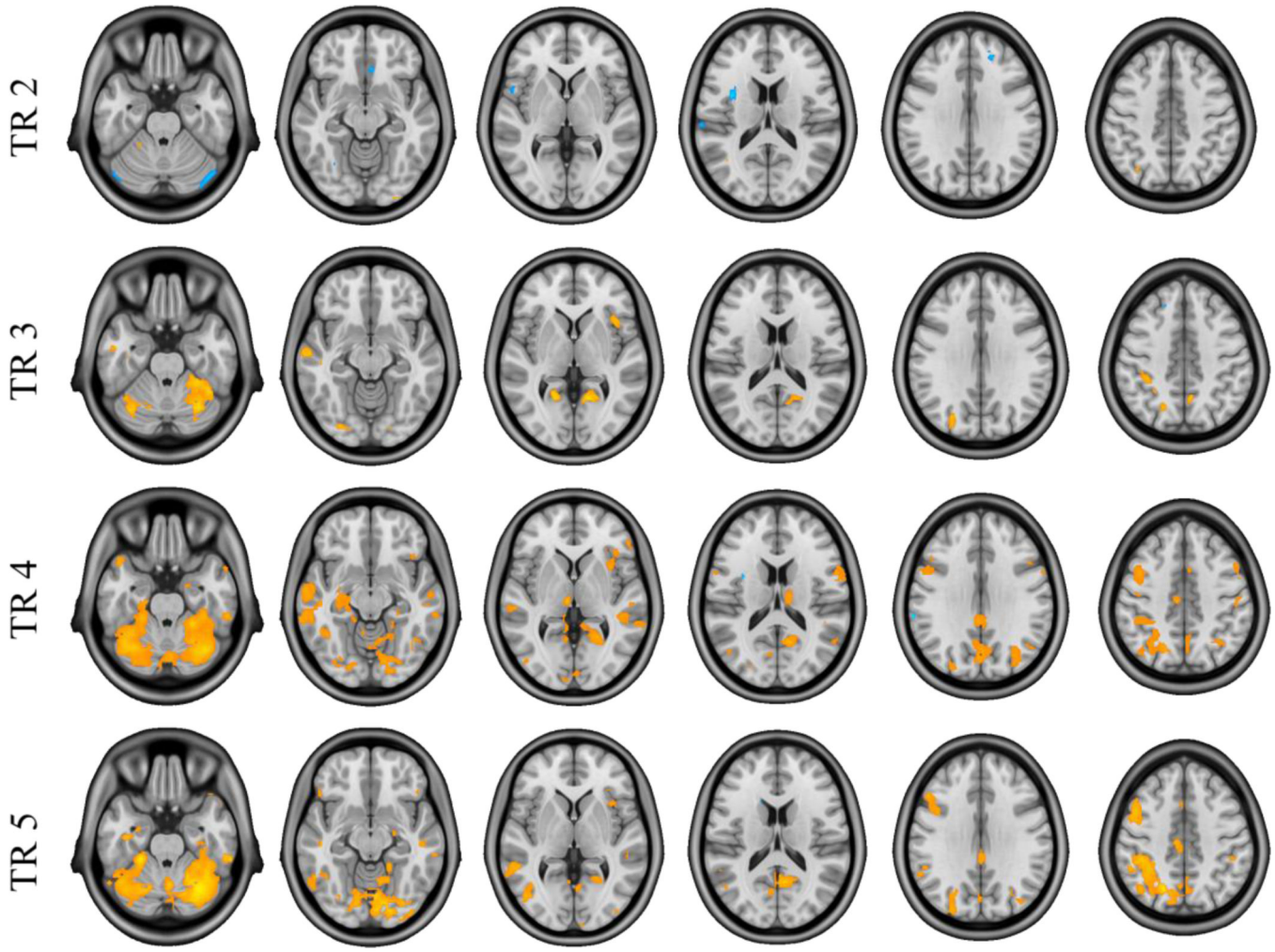

Figure 2. Results of the task PLS analysis comparing *Congruent* and *Incongruent* future simulation conditions

Images of activation at TRs 2-5, thresholded using a bootstrap ratio of ±3.00 (equivalent to $p < .001$) and an extent threshold of 10 voxels, superimposed on a standard anatomical template. Warm saliences correspond to areas associated with the *Congruent* condition and cool saliences with the *Incongruent* task.

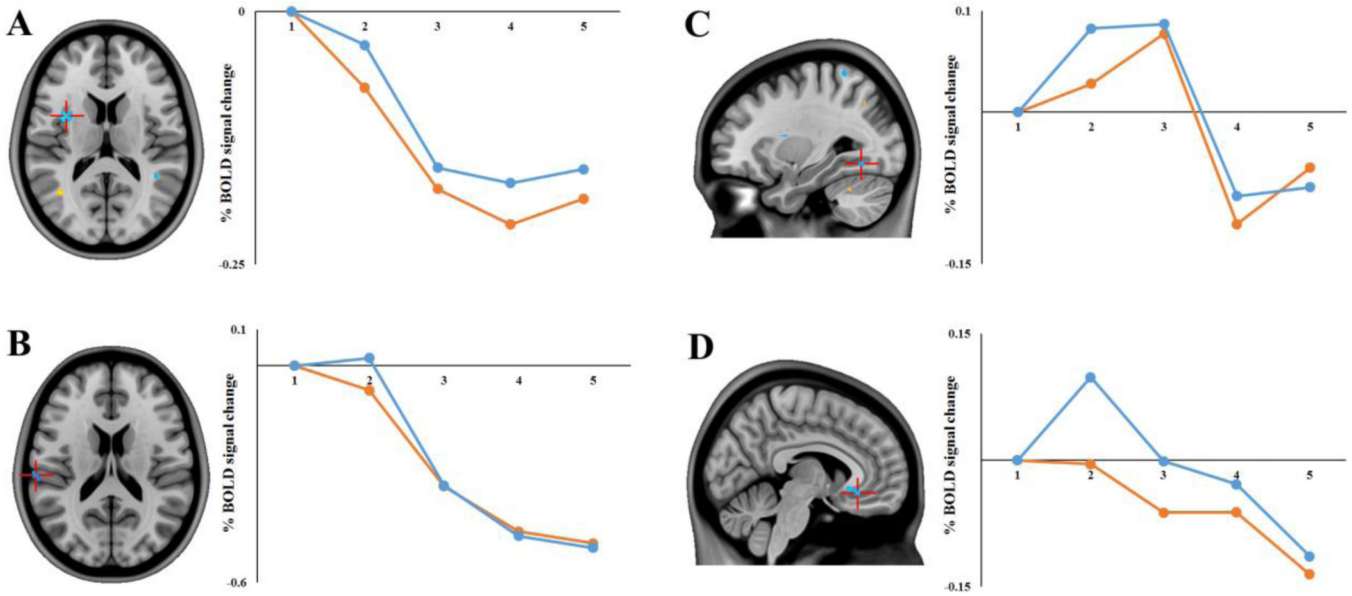

Figure 3. ***Incongruent > Congruent*** **Task PLS results in selected regions of interest**

Regions showing an *Incongruent* > *Congruent* effect (negative saliences/cool colors) at TR 2: **(A)** Left insula (*xyz* −38 4 14); **(B)** left supramarginal gyrus (*xyz* −64 −26 18); **(C)** left fusiform gyrus (*xyz* −30 −62 −10); and **(D)** right subcallosal cortex (*xyz* 6 30 −12). Images are thresholded using a bootstrap ratio of ±3.00 (equivalent to $p < .001$) and an extent threshold of 10 voxels, and are superimposed on a standard anatomical template. Plots show percent signal change (extracted from peak voxels) for each future simulation condition as a function of TR.

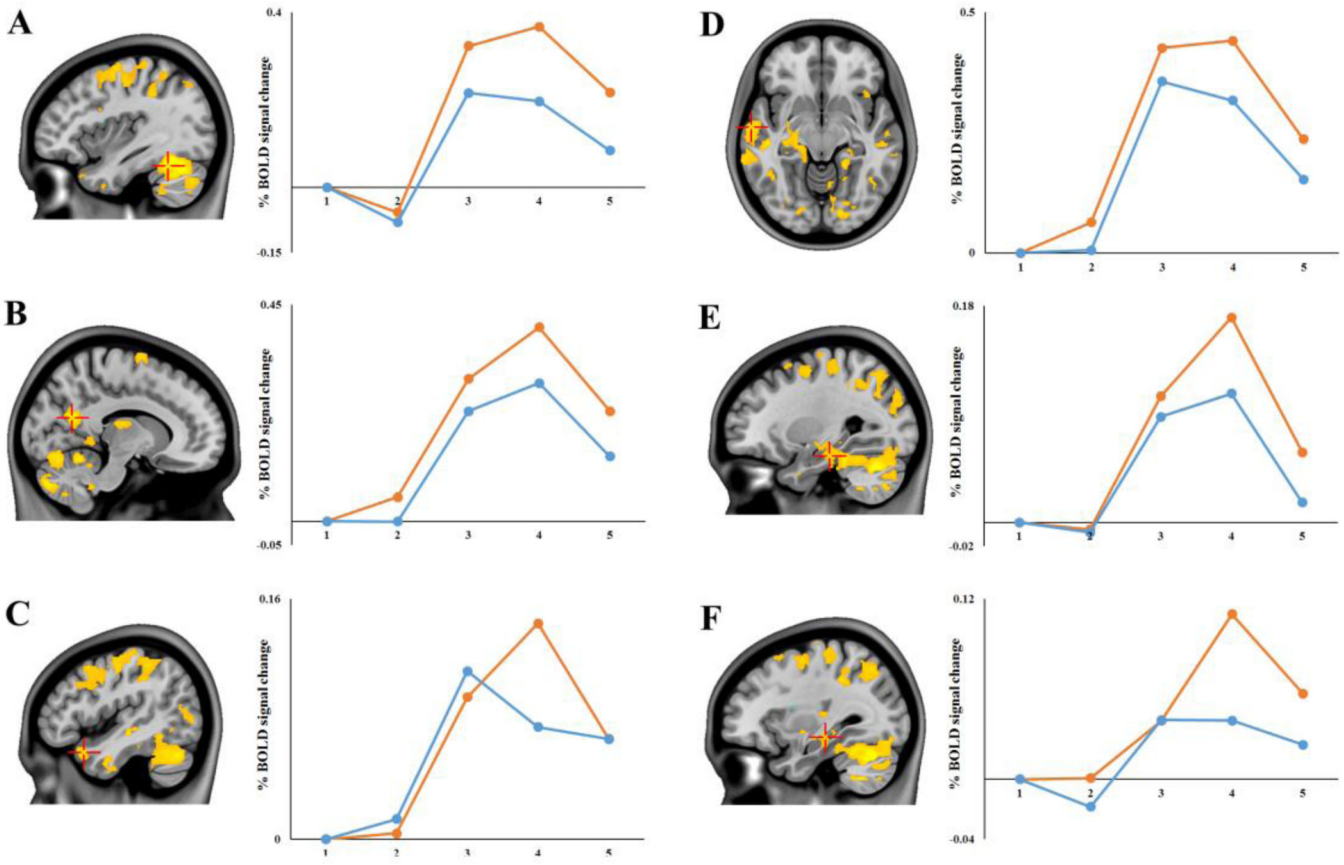

Figure 4. ***Congruent*** **>** ***Incongruent*** **Task PLS results in selected regions of interest**

Default mode network regions showing a *Congruent* > *Incongruent* effect (positive saliences/warm colors) at TR 4: **(A)** left cerebellum (*xyz* −38 −54 −22); **(B)** right precuneus (*xyz* 12 −62 20); **(C)** left temporal pole (*xyz* −46 16 −26); **(D)** left temporal pole (*xyz* −62 −10 −10); **(E)** left parahippocampal gyrus (*xyz* −28 −24 −20); and **(F)** left hippocampus (*xyz* −32 −24 −12) Images are thresholded using a bootstrap ratio of ±3.00 (equivalent to $p < .001$) and an extent threshold of 10 voxels, and are superimposed on a standard anatomical template. Plots show percent signal change (extracted from peak voxels) for each future simulation condition as a function of TR.

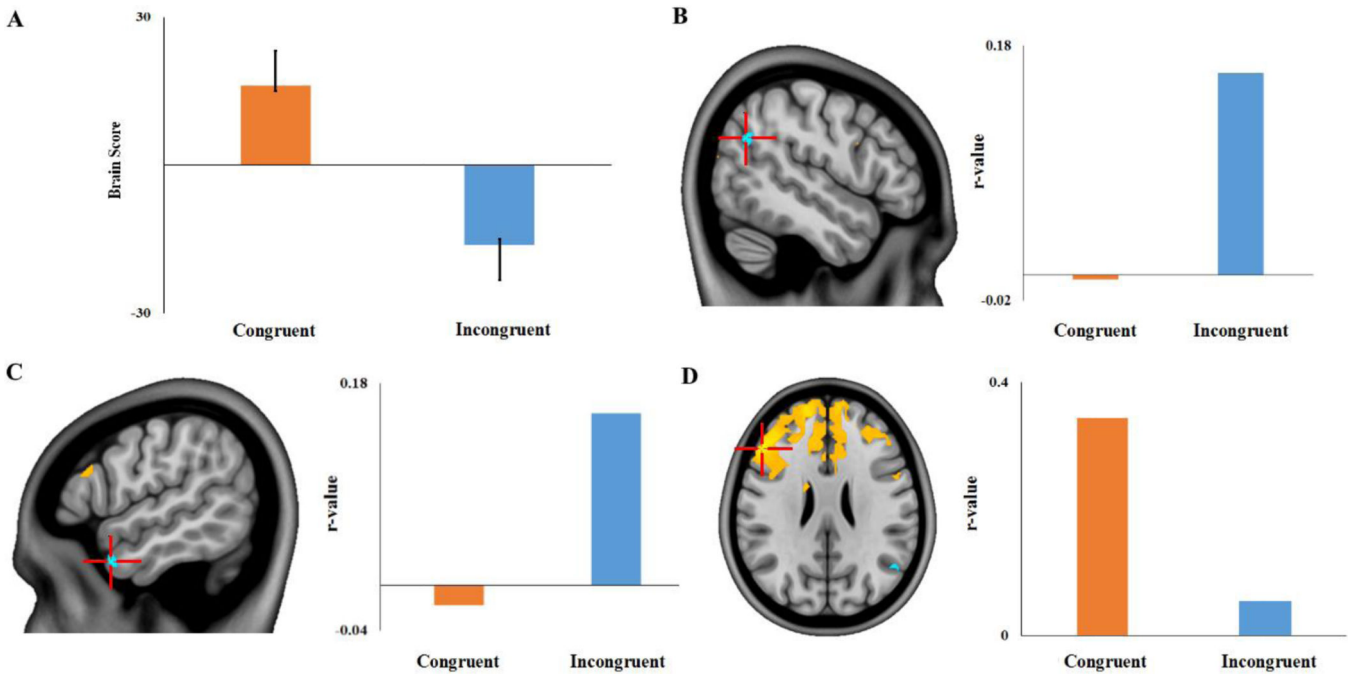

Figure 5. Within-subject seed PLS results

(A) A significant latent variable indicated that functional connectivity with the left mid-anterior insula seed (*xyz* −38 4 14) differed according to future simulation condition. Regions with negative saliences (cool colors) exhibited an *Incongruent* > *Congruent* effect, and included **(B)** right angular gyrus (*xyz* 50 −62 28) and **(C)** left temporal pole (*xyz* −56 8 −30). Regions with positive saliences (warm colors), such as **(D)** left dorsolateral prefrontal cortex (*xyz* −50 30 26), exhibited a *Congruent* > *Incongruent* effect. Images are thresholded using a bootstrap ratio of ±3.00 (equivalent to $p < .001$) and an extent threshold of 10 voxels, and are superimposed on a standard anatomical template. Plots show seed-voxel correlations (extracted from peak voxels) for each future simulation condition.

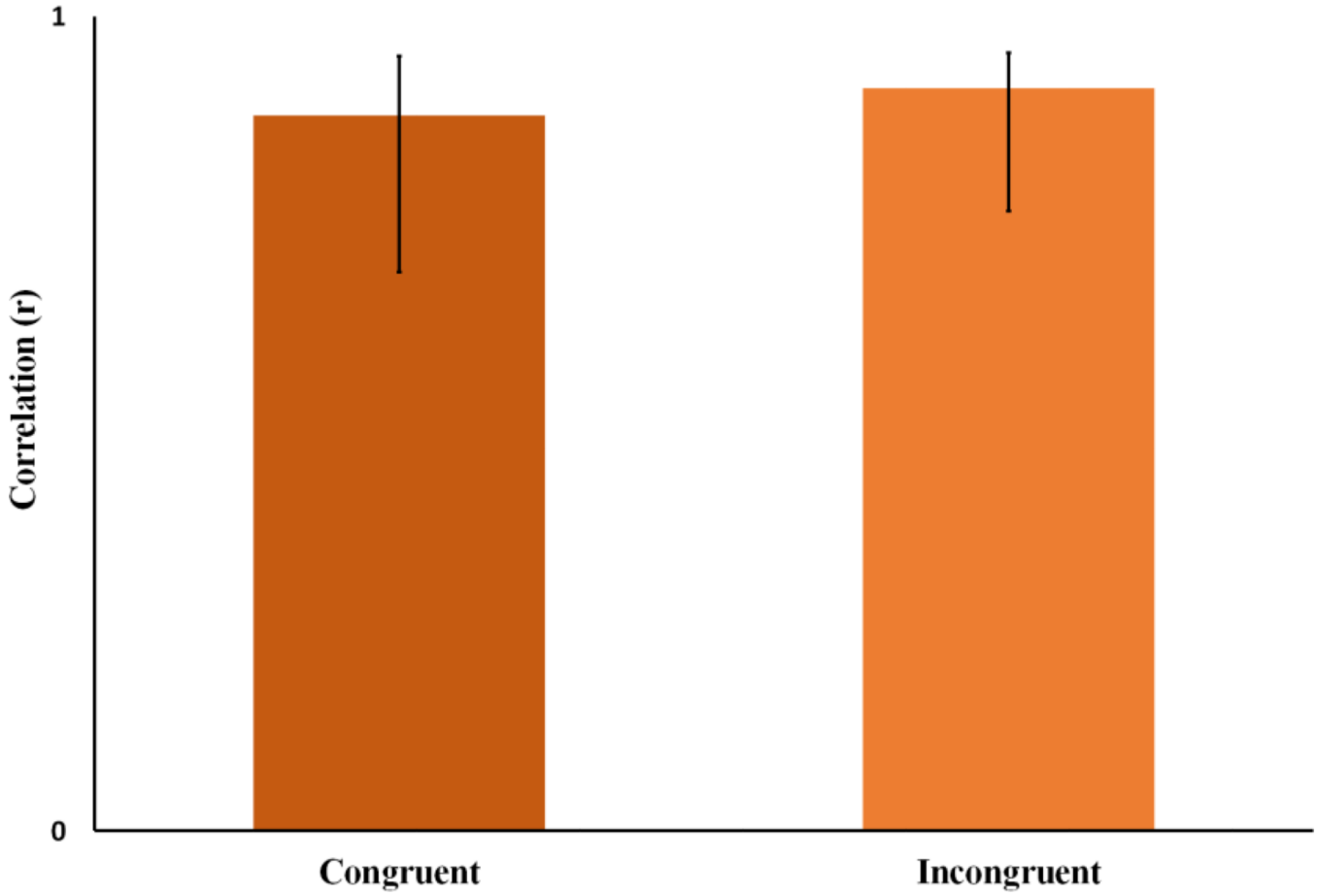

Figure 6. Behavior PLS results

This plot depicts the correlation profile for a significant latent variable showing correlations between AUT flexibility scores and brain scores during *Congruent* and *Incongruent* conditions.

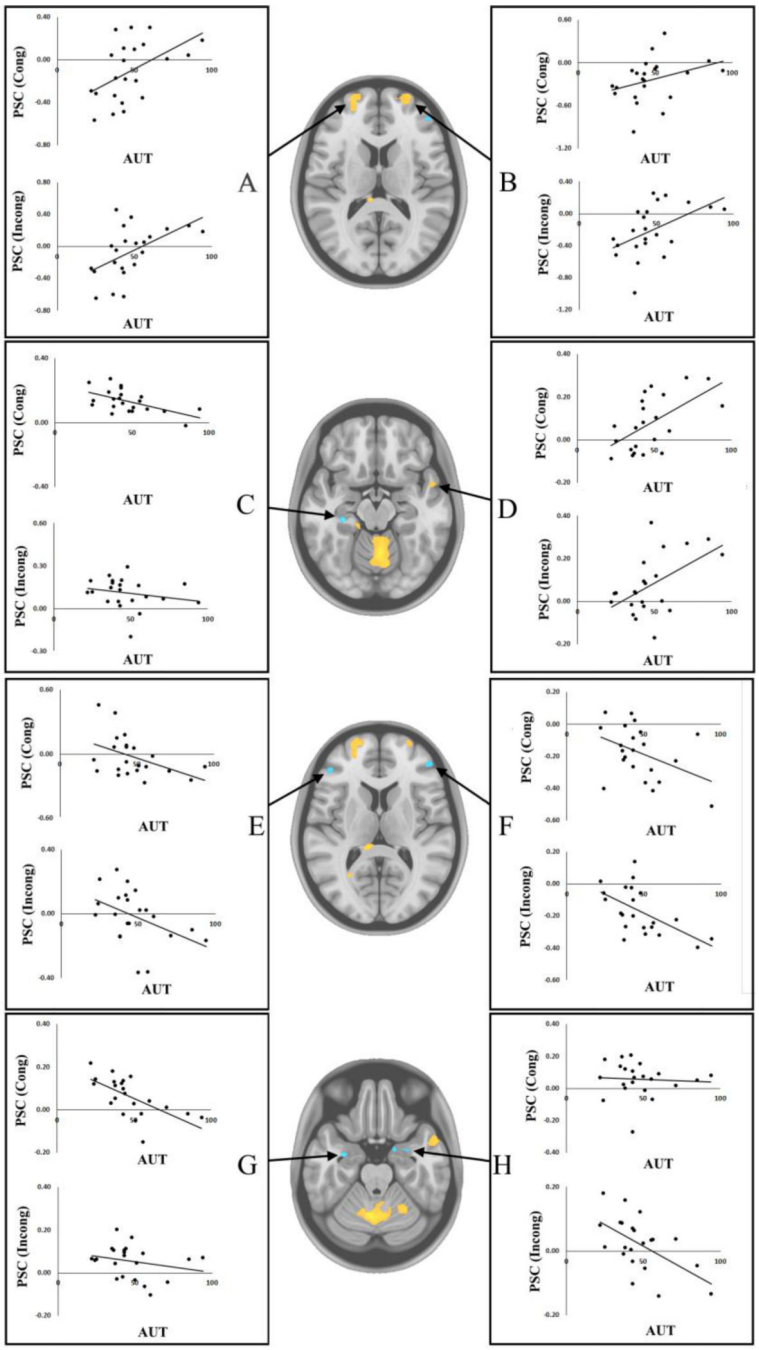

Figure 7. Behavior PLS results

Correlations of Alternate Uses Task flexibility score for *Congruent* and *Incongruent* conditions with BOLD signal from selected regions of interest: **(A)** Left rostrolateral prefrontal cortex (*xyz* −20 62 10); **(B)** right rostrolateral prefrontal cortex (*xyz* 24 60 16); **(C)** left hippocampus (*xyz* −30 −28 −16); **(D)** right temporal pole (*xyz* 52 4 −18); **(E)** left inferior frontal gyrus (*xyz* −46 38 8); **(F)** right ventrolateral prefrontal cortex (*xyz* 46 44 12); **(G)** left amygdala (*xyz* −32 −4 −24); **(H)** right amygdala (*xyz* 30 0 −26). Images are thresholded using a bootstrap ratio of ±3.00 (equivalent to $p < .001$) and an extent threshold

of 10 voxels, and are superimposed on a standard anatomical template. PSC = percent signal change; AUT = Alternate Uses Task flexibility scores; Cong = Congruent condition; Incong = Incongruent condition

Table 1

Behavioral and Phenomenological Measures for Future Simulation and Control Conditions

	Mean (SD)		
	Control Condition	**Congruent Future Condition**	**Incongruent Future Condition**
Number of trials *	44 (3)	39 (4)	34 (7)
Reaction Time (*s*) *	4.01 (0.90)	4.93 (1.11)	5.12 (1.18)
Likelihood of co-occurrence *†	n/a	1.00 (0.42)	0.42 (0.26)
Temporal distance (years)	n/a	1.53 (0.44)	1.66 (0.63)
Difficulty *†	n/a	0.93 (0.39)	1.24 (0.45)
Similarity to previous events *†	n/a	0.70 (0.48)	0.38 (0.38)
Plausibility *†	n/a	1.20 (0.46)	0.61 (0.31)
Detail *†	n/a	1.65 (0.34)	1.51 (0.37)
Subsequent cued-recall (proportion correct)	n/a	.60 (.16)	.48 (.20)

† *Note*. Rating scale (0–3) where 0 = low, and 3 = high.

* Significant difference between conditions ($p < .001$).

SD, standard deviation; *s*, seconds.

Table 2

Task PLS results: Negative and positive saliences associated with the *Congruent* and *Incongruent* future simulation conditions

Structure	Coordinates (MNI)			BSR	Cluster size (*k*)
	x	*y*	*z*		
(A) Incongruent > Congruent (TR 2)					
Default Mode Network					
R Subcallosal Cortex	6	30	−12	−4.26	33
Salience Network					
L Insula	−38	4	14	−6.40	53
L Supramarginal Gyrus	−64	−26	18	−4.33	29
Other Regions					
R Cerebellum	48	−74	−24	−4.65	213
L Middle Temporal Gyrus	−44	−46	6	−4.36	19
L Cerebellum	−46	−76	−26	−4.07	60
L Frontal Orbital Cortex	−20	28	−20	−4.07	47
L Fusiform Cortex	−30	−62	−10	−4.04	10
(B) Congruent > Incongruent (TR 2)					
Default Mode Network					
L Paracingulate Gyrus	−12	42	−2	4.37	16
R Middle Temporal Gyrus	56	−2	−22	4.26	21
R Precuneus/Posterior Cingulate Cortex	2	−54	26	3.53	11
Salience Network					
R Insula	40	14	−4	3.67	24
Other Regions					
R Occipital Pole	28	−98	−14	4.99	11
L Cerebellum	−18	−46	−22	4.27	64
L Middle Temporal Gyrus	−40	−60	12	4.11	25
(C) Incongruent > Congruent (TR4)					
Salience Network					
L Insula	−34	4	14	−3.82	10
(D) Congruent > Incongruent (TR 4)					

Structure	Coordinates (MNI)			BSR	Cluster size (*k*)
	x	*y*	*z*		
Default Mode Network					
L Cerebellum	−38	−54	−22	9.92	10841
extends into: R Precuneus	12	−62	20	7.07	
L Parahippocampal Gyrus	−28	−24	−20	4.58	
R Parahippocampal Gyrus	28	−24	−18	4.08	
L Hippocampus	−32	−24	−12	4.04	
R Inferior Temporal Gyrus	58	−34	−26	6.63	549
L Middle Temporal Gyrus	−48	−24	−8	6.05	876
extends into: L Temporal Pole	−62	−10	−10	4.89	
L Temporal Pole	−46	16	−26	5.48	152
R Superior Parietal Lobule/Angular Gyrus	28	−50	52	4.91	391
R Temporal Pole	56	12	−24	4.70	21
R Middle Temporal Gyrus	52	−8	−20	4.43	101
R Frontal Pole	52	36	2	4.38	18
L Inferior Temporal Gyrus	−46	−4	−36	4.23	97
R Middle Temporal Gyrus	52	2	−32	3.88	31
Frontoparietal Control Network					
L Superior Parietal Lobule	−18	−62	50	5.81	1300
R Middle Frontal Gyrus	36	26	20	4.32	10
R Middle Frontal Gyrus *D*	54	14	40	4.25	248
L Middle Temporal Gyrus	−66	−56	−4	3.89	62
Salience Network					
L Supplementary Motor Cortex	−4	6	54	5.49	396
R Insula *D*	34	16	10	5.08	353
R Supramarginal Gyrus	42	−44	22	4.97	28
L Precentral Gyrus	−8	−20	46	4.85	55
R Precentral Gyrus	58	4	14	4.47	197
R Superior Frontal Gyrus	12	0	76	4.43	780
R Insula	38	0	6	3.78	17
R Insula	42	−10	6	3.56	13

Structure	Coordinates (MNI)			BSR	Cluster size (*k*)
	x	*y*	*z*		
Other Regions					
L Thalamus	−6	−18	0	5.94	86
L Precentral Gyrus	−42	−12	54	5.35	1584
R Lateral Occipital Cortex	44	−68	−6	4.93	107
L Cerebellum	−10	−46	−50	4.91	183
R Temporal Pole	40	26	−34	4.80	20
L Parahippocampal Gyrus	−20	2	−34	4.64	56
R Cerebellum	10	−42	−42	4.57	44
L Precentral Gyrus	−40	6	24	4.42	38
R Thalamus	12	−18	14	4.25	108
R Superior Frontal Gyrus	20	−10	72	4.13	27
R Postcentral Gyrus	52	−18	44	4.13	33
L Lateral Occipital Cortex	−28	−84	30	4.01	108
L Occipital Pole	−14	−96	−2	3.96	172
L Lingual Gyrus	−6	−40	4	3.90	95
R Parahippocampal Gyrus	20	−6	−26	3.88	19
R Inferior Temporal Gyrus	48	−14	−42	3.42	11

Note. Bootstrap ratios were greater than ±3.00 (roughly equivalent to *p*-value <.001) and an extent threshold of 10 voxels was applied. *k* = number voxels comprising a cluster.

[D] Greater than 20% of cluster extended into default mode network.

BSR, bootstrap ratio; L, left; MNI, Montreal Neurological Institute; R, right.

Neuropsychologia. Author manuscript; available in PMC 2018 January 27.

Table 3

ws-seed PLS results: Negative and positive saliences exhibiting functional connectivity with the left insula during the *Congruent* and *Incongruent* conditions

Structure	Coordinates (MNI)			BSR	Cluster size (*k*)
	x	*y*	*z*		
(A) Incongruent > Congruent					
Default Mode Network					
L Temporal Pole	−56	8	−30	4.13	24
R Angular Gyrus	50	−62	28	3.76	37
Other Regions					
R Cerebellum	14	−46	−16	4.00	72
R Temporal Pole	32	6	−28	3.96	17
L Cerebellum	−16	−62	−44	3.68	14
R Cerebellum	12	−68	−40	3.64	24
L Cerebellum	−8	−68	−34	3.46	19
(B) Congruent > Incongruent					
Default Mode Network					
R Superior Frontal Gyrus	2	44	46	−5.28	2671
Medial Prefrontal Cortex	12	48	−8	−3.61	22
Frontoparietal Control Network					
L Middle Frontal Gyrus[D]	−50	30	26	−7.02	9188
L Frontal Pole	−28	44	−10	−6.31	252
Salience Network					
R Precentral Gyrus	56	8	28	−3.66	22
L Anterior Cingulate Cortex[F]	−2	−4	34	−3.54	17
Other Regions					
R Caudate	16	16	20	−6.70	141
L Precentral Gyrus	−36	−2	34	−5.07	32
L Caudate	−16	10	10	−5.04	751
R Lateral Occipital Cortex	48	−82	18	−4.31	14

Structure	Coordinates (MNI)			BSR	Cluster size (*k*)
	x	*y*	*z*		
L Caudate	−16	26	2	−3.89	19
B Medial Prefrontal Cortex	0	36	−26	−3.83	13
R Lateral Occipital Cortex	28	−58	48	−3.77	13
L Supramarginal Gyrus	−44	−34	36	−3.48	20

Note. Bootstrap ratios were greater than ±3.00 (roughly equivalent to $p < .001$) and an extent threshold of 10 voxels was applied. *k* = number voxels comprising a cluster.

^{D}Greater than 20% of cluster extended into default mode network.

^{F}Greater than 20% of cluster extended into frontoparietal control network.

B, bilateral; BSR, bootstrap ratio; L, left; MNI, Montreal Neurological Institute; R, right.

Table 4

Behavior PLS results: Negative and positive saliences correlated with Alternate Uses Task flexibility scores

Structure	Coordinates (MNI)			BSR	Cluster size (*k*)
	x	*y*	*z*		
(A) Positively correlated with AUT flexibility scores (TR 3)					
Default Mode Network					
L Rostrolateral Prefrontal Cortex[F]	−20	62	10	4.64	155
R Superior Temporal Gyrus/Temporal Pole	52	4	−18	4.46	121
R Rostrolateral Prefrontal Cortex[F]	24	60	16	4.24	115
R Superior Frontal Gyrus	22	18	42	3.76	14
Frontoparietal Network					
R Lateral Occipital Cortex	24	−84	48	6.60	117
R Superior Frontal Gyrus	30	−4	64	4.13	33
Salience Network					
L Paracingulate Gyrus	−12	10	42	3.62	14
Other Regions					
L Cerebellum	−6	−62	−26	7.59	1341
L Superior Frontal Gyrus	−20	−2	50	5.73	103
L Thalamus	−10	−34	12	5.63	52
L Superior Parietal Lobule	−30	−58	60	5.56	35
L Precuneus	−30	−60	6	5.47	129
R Superior Frontal Gyrus	24	0	48	5.23	56
L Occipital Pole	−38	−94	0	4.67	37
R Cerebellum	26	−56	−24	4.60	77
R Intracalcarine Cortex	30	−60	2	4.57	136
R Inferior Temporal Gyrus	56	−26	−30	4.43	10
R Lateral Occipital Cortex	36	−82	0	4.26	54
R Postcentral Gyrus	54	−12	38	3.82	27
R Caudate	16	12	18	3.58	16
L Parahippocampal Gyrus	−18	−32	−16	3.51	18
R Cerebellum	14	−36	−20	3.35	12

Structure	Coordinates (MNI)			BSR	Cluster size (*k*)
	x	*y*	*z*		
(B) Negatively correlated with AUT flexibility scores (TR 3)					
Default Mode Network					
L Hippocampus	−30	−28	−16	−5.80	17
Frontoparietal Network					
L Middle Frontal Gyrus	−50	14	44	−4.45	36
L Inferior Frontal Gyrus	−46	38	8	−4.41	21
R Ventrolateral Prefrontal Cortex	46	44	12	−3.95	33
Salience Network					
L Insula	−40	4	−8	−3.99	14
Other Regions					
R Postcentral Gyrus	56	−16	54	−5.65	28
L Amygdala	−32	−4	−24	−5.33	18
R Amygdala	30	0	−26	−3.90	10
R Parahippocampal Gyrus	16	2	−24	−3.89	14

Note. Bootstrap ratios were greater than ±3.00 (roughly equivalent to a *p*-value of <.001) and an extent threshold of 10 voxels was applied. *k* = number voxels comprising a cluster.

F Greater than 20% of cluster extended into frontoparietal control network.

AUT, Alternate Uses Task; BSR, bootstrap ratio; L, left; MNI, Montreal Neurological Institute; R, right.